# CYTOTOXIC EFFECT OF KONJAC GLUCOMANNAN ON THE MOLECULAR AND DIELECTRIC PROPERTIES OF HEPG2 AND WRL68 LIVER CELL LINES

**SAKUNIE A/P SAWAI**



**FACULTY OF ENGINEERING**
**UNIVERSITY OF MALAYA**
**KUALA LUMPUR**

**2019**

# CYTOTOXIC EFFECT OF KONJAC GLUCOMANNAN ON THE MOLECULAR AND DIELECTRIC PROPERTIES OF HEPG2 AND WRL68 LIVER CELL LINES

SAKUNIE A/P SAWAI

DISSERTATION SUBMITTED IN FULFILMENT
OF THE REQUIREMENTS FOR THE DEGREE OF
MASTER OF ENGINEERING SCIENCE

FACULTY OF ENGINEERING
UNIVERSITY OF MALAYA

2019

**UNIVERSITI MALAYA**

**ORIGINAL LITERARY WORK DECLARATION**

Name of Candidate: **Sakunie A/P Sawai**
Registration/Matric No: **KGA150089**
Name of Degree: **Master of Engineering Science**
Title of Project Paper/Research Report/Dissertation/Thesis ("this Work"): **Cytotoxic Effect of Konjac Glucomannan on the Molecular and Dielectric Properties of HepG2 and WRL68 Liver Cell Lines**
Field of Study: **Biomedical Engineering**

I do solemnly and sincerely declare that:
(1) I am the sole author/writer of this Work;
(2) This Work is original;
(3) Any use of any work in which copyright exists was done by way of fair dealing and for permitted purposes and any excerpt or extract from, or reference to or reproduction of any copyright work has been disclosed expressly and sufficiently and the title of the Work and its authorship have been acknowledged in this Work;
(4) I do not have any actual knowledge nor do I ought reasonably to know that the making of this work constitutes an infringement of any copyright work;
(5) I hereby assign all and every rights in the copyright to this Work to the University of Malaya ("UM"), who henceforth shall be owner of the copyright in this Work and that any reproduction or use in any form or by any means whatsoever is prohibited without the written consent of UM having been first had and obtained;
(6) I am fully aware that if in the course of making this Work I have infringed any copyright whether intentionally or otherwise, I may be subject to legal action or any other action as may be determined by UM.

Candidate's Signature Date

Subscribed and solemnly declared before,

Witness's Signature Date
Name:
Designation:

# CYTOTOXIC EFFECT OF KONJAC GLUCOMANNAN ON THE MOLECULAR AND DIELECTRIC PROPERTIES OF HEPG2 AND WRL68 LIVER CELL LINES


## ABSTRACT

Hepatocellular carcinoma (HCC) is the most lethal hepatic cancer type in both men and women worldwide due to late diagnosis, inefficient therapeutic outcomes with many side effects as well as disease recurrence. Hence, investigating safer and effective cancer treatment alternative for liver cancer using natural product is the main focus of the present study. Konjac glucomannan (KGM), a water-soluble dietary fibre of *Amorphophallus konjac* K. Koch has been clinically proven as an effective antioxidant, anti-microbial and laxative agent, intriguingly it is traditionally known for its tumour suppression and prevention properties which remain to be explored. This study thus aimed to determine the potential cytotoxic effect of KGM on hepatic carcinoma cell line, HepG2 and non-malignant hepatic cell line, WRL68 (control) for their viability, proliferation and dielectric properties using molecular and dielectrophoresis biosensor techniques. KGM treatment at the concentration of 3.60 mg/mL resulted in reduced viability of HepG2 cells significantly, in line with the apoptotic-like morphological changes, while WRL68 cell viability remained unaffected. High BAX to BCL2 gene expression ratio suggests that KGM inhibits HepG2 cell viability via activation of Bcl-2/BAX protein pathway. Meanwhile, standard chemo-drug, 5-Fluorouracil (5-FU) remains effectual against HepG2 cells; it does not confer selective inhibition, since the treatment affects the viability of both HepG2 and WRL68 cell lines. In addition, KGM disrupted the dielectric qualities of HepG2 surface membrane which cells undergo apoptosis and experienced p-DEP at crossover frequency (220 kHz). Comparative monosaccharide D-mannose used in this study showed no significant inhibition but rather supported the growth and proliferation of both cell lines, suggesting that

compounds from saccharide family do not always inhibit the cancer cell viability or may involve in different inhibition pathways. Overall, selective cytotoxic effect of KGM on HepG2 cells viability, proliferation and dielectric properties suggested KGM as a potential anti-cancer entity to be further studied for its therapeutic uses.

**Keywords:** hepatocellular carcinoma, konjac glucomannan, cytotoxicity, apoptosis, dielectric property

# KESAN SITOTOKSIK KONJAC GLUCOMANNAN TERHADAP CIRI-CIRI MOLEKULAR DAN DIELEKTRIK SEL HATI HEPG2 DAN WRL68


## ABSTRAK

Karsinoma hepatoselular (HCC) merupakan barah hati yang paling kerap didiagnosis di dunia. Kadar kematian yang tinggi dalam kalangan pesakit HCC disebabkan oleh ketumbuhan hanya dapat didiagnosis pada peringkat akhir, ketidakberkesanan terapi serta ketumbuhan ulangan. Maka, ejen anti-kanser sebagai rawatan alternatif kepada kanser hati menjadi fokus utama kajian ini. Konjac glucomannan (KGM), sejenis serat larut air daripada *Amorphophallus konjac* K. Koch telah terbukti secara klinikal sebagai antioksidan, anti-mikrob serta ejen pelawas. Namum ciri-ciri anti-tumor yang diketahui umum masih belum diterokai. Objektif kajian ini adalah untuk mengkaji kesan sitotoksik rawatan KGM terhadap sel HepG2 serta WRL68 menggunakan kaedah molekular dan biosensor DEP. Berdasarkan keputusan kajian, rawatan KGM menunjukkan penurunan bilangan sel HepG2 bersertakan perubahan morfologi yang ketara. Nisbah BAX:BCL2 yang tinggi melalui analisa gen menyokong keberangkalian kesan KGM terhadap sel HepG2 adalah melalui sistem protein Bcl-2/BAX. Penggunaan ejen kemoterapi, 5-FU menghasilkan kesan yang paling berkesan terhadap sel HepG2, namum ia tidak menunjukkan kesan selektif sepertimana KGM. Selain itu, KGM juga mengganggu fungsi selular dan kestabilan dielektrik pada permukaan sel HepG2, menghasilkan kesan DEP positif pada frekuensi *crossover* (220 kHz). Sebaliknya, D-mannose tidak menunjukkan perubahan molecular dan dielektrik yang ketara terhadap kedua-dua jenis sel. Keseluruhannya, KGM berpotensi sebagai ejen anti-kanser yang selamat digunakan untuk mencegah pertumbuhan tumor hati.



**Kata kunci:** karsinoma hepatoselular, konjac glucomannan, kesan sitotoksik, *apoptosis*, sifat dielektrik

## ACKNOWLEDGEMENTS

My foremost sincere gratitude goes to my supervisor, Ir. Dr. Mas Sahidayana Mohktar, together with her advisor, Prof. Ir. Dr. Fatimah Ibrahim, of Department of Biomedical Engineering, Faculty of Engineering, for giving me the opportunity to be part of their research team. This project, however, would have been impossible without another two incredible co-supervisors, Dr. Wan Safwani Wan Kamarul Zaman of Department of Biomedical Engineering, Faculty of Engineering, and Dr. Thamil Selvee Ramasamy of Department of Molecular Medicine, Faculty of Medicine. Their endless supports, priceless guidance and mutual dedications greatly empower the achievement of the research milestones.

My heartfelt appreciation is dedicated to the University of Malaya Research Grant (Project numbers: RP022C-14AFR and RP040B-15HTM) and the Postgraduate Research Grant (PG072-2016A) for funding this research. With a special mention to Miss Ainul Bashirah Marzuke, Miss Ain Zubaidah Ayob, Miss Nor Shiham Abdul Rashid, Centre for Innovation in Medical Engineering, Department of Biomedical Engineering, Department of Molecular Medicine, Stem Cell Biology Laboratory, MBL and CAREF, for providing facilities and assistances in completion of my work.

I would also like to acknowledge both internal and external examiners for reviewing my dissertation. Your valuable comments are surely helpful in improving the quality of my write-up. Finally, my profound gratitude goes to my beloved family and friends. This accomplishment would not have been possible without their unfailing supports and continuous encouragement throughout the years of my study. Sincerely, thank you.

## TABLE OF CONTENTS

## LIST OF FIGURES

## LIST OF TABLES

## LIST OF SYMBOLS AND ABBREVIATIONS

| | |
|---|---|
| µS/cm | Microsiemens per centimetre |
| 5-FU | 5-fluouracil |
| ACC | Acetyl-CoA carboxylase |
| AFP | α-fetoprotein |
| ATP | Adenosine triphosphate |
| BAX | Bcl-2-associated X protein |
| BCL2 | B-cell lymphoma 2 regulatory proteins |
| bFGF | Basic fibroblast growth factor |
| CDK | Cyclin-dependent kinase |
| CGM | Complete growth medium |
| CPT1 | Carnitine palmitoyltransferase 1 |
| CT | Computed tomography |
| DEP | Dielctrophoresis |
| DMEM | Dulbecco's modified eagle medium |
| ECM | Extracellular matrix |
| FA | Fatty acid |
| FBS | Foetal bovine serum |
| FITC | Fluorescein isothiocyanate |
| G | Gravity force |
| HCC | Hepatocellular carcinoma |
| HepG2 | Human cancer liver cell line |
| $IC_{50}$ | Half maximal inhibitory concentration |
| Igf | Insulin-like growth factor |
| ITO | Indium tin oxide |

| | |
|---|---|
| KCl | Potassium chloride |
| kDa | Kilodalton |
| KGM | Konjac glucomannan |
| LDL | Low density lipoprotein |
| LOC | Lab-on-a-chip |
| MDA | Malondialdehyde |
| MRI | Magnetic resonance imaging |
| MTT | 3-(4,5-dimethylthiazol-2-yl)-2,5-diphenyltetrazolium bromide |
| OLT | Orthotopic liver transplantation |
| PBS | Phosphate buffer saline |
| PCR | Polymerase chain reaction |
| PI | Propidium iodide |
| POC | Point-of-care |
| Pten | Phosphatase and tensin homolog |
| qPCR | Real-time polymerase chain reaction |
| RB | Retinoblastoma protein |
| rpm | Revolutions per minute |
| Shp2 | SH2-containing tyrosine phosphatase |
| TACE | Transarterial chemoembolisation |
| TG | Triglyceride |
| TSG | Tumour suppressive protein-coding gene |
| VEGF | Vascular endothelial growth factor |
| WRL68 | Human normal liver cell line |

## LIST OF APPENDICES

# CHAPTER 1

# INTRODUCTION

This chapter introduces the significant concern on the current hepatocellular carcinoma (HCC) occurrence worldwide. The research problems include the challenges and limitations in diagnosis and treatment of HCC. Based on the focused research problems, this chapter further describes the outline, overall aim and specific objectives of this study.

## 1.1 Background

### 1.1.1 Liver Cancer

Liver malignancy is the seventh most diagnosed cancer and the second cancer-related death in men in 2012 worldwide (International Agency for Research on Cancer, 2016). Hepatocellular carcinoma (HCC) is one of the most lethal liver malignancies in both men and women. The incidences of HCC are most prevalent in developing countries of Asia and Africa, but in the past decade, it shown increasing incidence in Western Europe as well as the United States (Darvesh, Aggarwal & Bishayee, 2012). In 2012, World Health Organization (WHO) reported 782,451 new liver cancer cases diagnosed worldwide with only 2.0% survival rate. In Malaysia, the age-standardised incidence and mortality rate of HCC in 2012 for both sexes were 1,527 and 1,750 per 100,000, respectively (International Agency for Research on Cancer, 2016). High mortality rate of HCC patients is mainly due to late diagnosis as the symptoms only arise at the

advanced stage leading to a major challenge in treating the cancer as often the treatment outcomes are not satisfactory and incurable (Zhao, Ju & Li, 2013).

## 1.2 Research Problems and Significance

### 1.2.1 Diagnosis of Liver Cancer: Current Practices and Challenges

Studies had shown that early diagnoses significantly improve the survival benefits and decrease the recurrent incidence among the liver cancer patients (Chiao, Yang & Frenette, 2013). To improve the survival rate and increase the chance of intervention, early detection of subclinical HCC by ultrasonography and α-fetoprotein (AFP) screening is implemented in several countries. These screening methods help detecting tumours at primary stage; increase the chance of receiving treatments.

A surveillance programme was done by Hepatitis clinic of the Queen Mary Hospital in Hong Kong, involving a total of 306 patients screened using AFP and ultrasonography methods for three years. The study shows that 142 asymptomatic patients were identified to have subclinical HCC and 164 patients diagnosed with symptomatic HCC. A total of 51 patients (38 subclinical and 13 symptomatic HCC) underwent curative resection; 117 patients (64 subclinical and 53 symptomatic HCC) received transarterial chemoembolisation (TACE); 4 patients (3 subclinical and 1 symptomatic HCC) received percutaneous ethanol injection; and 134 patients (37 subclinical and 97 symptomatic HCC) were treated with conservative chemotherapy. Patients treated via curative resection showed definitive survival advantage followed by TACE. Postresection tumour recurrence rate in subclinical HCC patients reduced significantly as compared to those symptomatic ones (Yuen et al., 2000).

Despite multiple diagnosis methods for liver cancer, as many other cancers, for instance physical examination, blood tests, ultrasound, computed tomography (CT) scan, magnetic resonance imaging (MRI), laparoscopy, angiogram and liver biopsy, yet these techniques often possess many limitations (Kudo, 2015). The conventional blood tests and ultrasound are the most commonly used methods in most hospital; however, it was exceedingly difficult to detect small abnormalities in liver which make early detection of liver cancer virtually impossible. On the other hand, techniques namely angiogram, laparoscopy and liver biopsy might provide more promising diagnosis and yet they are not very practical due to invasiveness and time consuming (Kudo, 2015). The advance technologies CT scanning and MRI are highly sensitive and detect the abnormalities at earlier stage but these techniques are exorbitantly expensive (Nam, Barrack & Potter, 2014). Furthermore, the carcinogenic potential associated with delivery and usage of high dose radiation by CT scanning remains as a major drawback of this test (Fred, 2004). Thus, investigation of effective tools for rapid diagnosis of liver cancer which offer safer alternatives to the current diagnosis techniques is essential.

### 1.2.2 Treatment of Liver Cancer: Current Practices and Challenges

Furthermore, there are several treatment options available namely chemotherapy, radiotherapy, liver transplantation, curative resection, trans-arterial chemoembolization and systemic targeted agents like sorafenib (Yuen et al., 2000). However, the effectiveness of these treatments is highly dependent on the stage of cancer progression, patient health status, and degree of liver-function impairment as well as the requirement for multimode therapeutic approaches. Significant developments in surgical and localised treatments improve the short-term survival rate; yet, the disease recurrence and relapse remain a major concern (Raza & Soob, 2014).

The conventional chemotherapy has shown to increase the survival rate of those cancer patients at early stages of cancer progression, meanwhile prolongs the survival of those with advanced and metastatic tumours. This however, is a double-edged sword with undesirable side effects namely fatigue, hair loss, infection, nausea and vomiting, changes in appetite, short concentration and focus, which impairs the overall healing capacity post-chemotherapy cycles (American Cancer Society, 2016). Fundamentally, chemotherapeutic drugs induce severe liver dysfunction due to drug toxicity and structural changes of liver tissue, leading to development of steatosis, chemotherapy-associated steatohepatitis (CASH) or hepatic sinusoidal obstruction syndrome (SOS) (Maor & Malnick, 2013).

A research team at University of California School of Medicine, San Diego, recently discovered the drawbacks of using chemotherapeutic drug in treating liver cancer. Current challenges of chemotherapy include unspecific targets by affecting both cancer and normal healthy cells causes side effects, survival rate is limited to patients and stages of cancer, development of resistance and exorbitant cost (Marur & Forastiere, 2010). Zhu et al. (2015) reported the vital role of two enzymes phosphatase and tensin homolog (Pten) and SH2-containing tyrosine phosphatase (Shp2) in prognosis of hepatic neoplasm. Pten is a tumour suppressor protein that was found overexpressed in large number of cancers due to the mutation in its encoding gene PTEN (Yin & Shen, 2008). Shp2 enzyme regulates numerous cellular activities namely cell growth and proliferation, differentiation and oncogenic transformation in which the mutation of the PTPN11 gene encoding this enzyme was found to be widely associated with development of several cancers (Stein-Gerlach, Wallasch & Ultrich, 1998). Several drug approaches act by inhibiting the activation of these enzymes; however, it had been proven to be ineffective against liver cancer. Their findings suggested that suppression

of Pten and Shp2 leads to liver damage and overtime, cancer, which associated with the poor prognosis of liver malignancies (Zhu et al., 2015).

The drawbacks of current treatment approaches draw broad interest among the researchers on natural product studies for cancer prevention and treatment. Many researches on natural products had been conducted in the past few decades especially those derived from plant sources due to easily accessible, cost-effective and more selective action towards cancer cells. Since ancient time, plants are used as food source and about 80 to 85% of the world populations especially in the developing countries rely mainly on plant as their primary health care (Prakash et al., 2013).

Several naturophatic agents had been introduced in liver cancer treatment namely minor bupleurum (dragon herb), silymarin and long pepper. Despite the therapeutic effectiveness of these natural agents, yet some intensify the liver impairment (Xiong & Guan, 2017). Food and Drug Administration (FDA) approved minor bupleurum as the first herbal drug for liver cirrhosis and chronic hepatitis treatment, yet it had been proven to cause long-term acute respiratory failure and severe interstitial pneumonia. In addition, its protective mechanism against liver fibrosis and HCC remains uncertain (Lee, Kim & Shin, 2011). Silymarin and long pepper are safer to consume except they induce allergic reactions, gastrointestinal symptoms and are not recommended during pregnancy and lactation (Bahmani et al., 2015; Kumar, Kamboj & Suman, 2011). These limitations and negative impacts hence warrant further improvements or safer substitute natural treatments.

## 1.3 Research Approaches

The limitations of liver cancer diagnoses and treatments were the major concern of this study. Therefore, konjac glucomannan (KGM), a safer plant-derived anti-cancer compound and dielectrophoresis (DEP) device, a portable and highly sensitive tool had been introduced. *Amorphophallus konjac* K. Koch was assessed for its anti-tumour properties on liver cancer cell line in this study. *A. konjac* commonly known as konjac, is one of the natural products that gained interest among the researchers to further study its medicinal properties. Konjac served as both food sources and traditional medicines in ancient Chinese, Japanese and South East Asian. In traditional Chinese medicine, the konjac flour gel was used for numerous courses such as detoxification, tumour-suppression, systemic circulation balance as well as respiratory tracts and skin disorders treatments (Chua et al., 2010).

Supplementing the diet with purified konjac flour or KGM has been clinically proven to significantly lower the plasma cholesterol, improves bowel movement and colonic ecology, and enhances carbohydrate metabolism (Chua et al., 2010). A study on protective role of KGM on human colon carcinogenesis by Chen *et al.,* (2011) reported that 4.5 g/day KGM supplemented diet improved faecal microbial ecology resulting in decreased production of β-glucuronidase enzyme that involved in toxin formation in colon. Reduction in faecal water toxicity minimised the precancerous risk of colorectal cancer. However, the tumour-suppression effect of KGM and its mechanism of action on cancer cells are not fully elucidated. Therefore, this research aimed at elucidating the cytotoxic effect of KGM, D-mannose, KGM-D-mannose combination and 5-fluouracil (5-FU) on the viability and proliferation of human normal (WRL68) and cancer (HepG2) liver cell lines. Monosaccharide D-mannose was used in this study as a comparative compound of KGM supported that this konjac fibre may be involved in the

activation of mannose binding receptors and its underlying cell death mechanism (Shahbuddin et al., 2013), while standard chemotherapeutic drug 5-FU served as positive control of the study.

Apart from assessing safer alternative treatment method, it is worth to as well explore new diagnostic tools which aid in detecting liver cancer at early stage. In the past two decades, researchers had gained wide interest toward point-of-care (POC) systems. POC system is a significant advance that can potentially improve the quality of care in a more patient-centred manner, as well as system remodelling (John & Price, 2013). POC is safer, faster and more specific, but of similar sensitivity to the formal laboratory screening approaches. POC may be possible to initiate treatment sooner when compared to a laboratory-based process, which give rise to better health outcomes (Chiao, Yang & Frenette, 2013).

High demand for rapid, reliable and cost-effective diagnostic procedures plays a major influence in development of advanced tools to replace the current laboratory-based diagnostic approaches that can only be conducted in fully equipped setting. Furthermore, portable miniaturised device which generates better reaction productivity, immediate results, low reagents or samples consumption is correspondingly vital (Yafouz, Kadri & Ibrahim, 2013). In this study, DEP biosensor technique was utilised to differentiate the cancerous cells from the normal as well as analysing the effects of KGM, D-mannose, KGM-D-mannose and standard drug 5-FU (positive control) treatments by determining the changes in cell membrane dielectric forces. This technique was implemented in complement with the bioassays accessing changes in molecular and cellular characteristics in both normal (WRL68) and cancer (HepG2) liver cell lines.

DEP is an advance technology manipulating and analysing the electrophysiological changes in bioparticles upon application of non-uniform electric fields from a special electrode (Yafouz, Kadri & Ibrahim, 2013). Applying electrical forces at the micro level allows researchers to identify the forces generated on cells depending on their electrical phenotype. This is useful in determining the electrical properties of a cell namely conductivity and permittivity, primarily via the total net charge and polarisability of the cells which generated "DEP spectrum" when applied with a specific signal frequency. Electrical phenotypes correlate to biological variations in cells for instance during cellular apoptosis and necrosis (Yafouz, Kadri & Ibrahim, 2013). Tissue electrical conductivity is valuable to determine the displacement of electromagnetic energy on the cell membrane and diagnostically differentiate between normal and neoplastic tissues (Haemmerich et al., 2003).

For instance, a study conducted by Graham et al. (2015) showed that DEP successfully discriminated the brush biopsy cancerous oral cells from the healthy oral epithelium with 81.6% sensitivity and 81.0% specificity, respectively. Cells experience different electrophysiological states at different stages of cancer and respond differently at the same range of frequencies and applied voltage. Rapid detection of electrophysiological changes in cells and the tag-free nature of DEP technique make it an ideal tool for cell membrane properties analysis, especially in diseases with unknown or inconsistent expression of biomarkers (Broche et al., 2007; Mulhall et al., 2011).

## 1.4 Aim and Objectives

The overall aim of this study is to elucidate the traditionally known potential tumour suppression property of KGM by assessing its effects on (i) cell viability and

proliferation through cytotoxicity assay, (ii) induction of apoptosis, (iii) modulation of proliferation and apoptotic genes expression, and (iv) alterations of cell membrane charges in HepG2 and WRL68 cells, using complemented molecular bioassays and DEP biosensor techniques. The objectives of the study are as follow,

Main objective:

To investigate the cytotoxic effect of KGM on normal (WRL68) and cancerous (HepG2) human liver cell lines by evaluating the molecular and dielectric characteristics.

Specific objectives:

1. To assess the morphological changes in HepG2 and WRL68 cells after treatments,
2. To determine the half maximal inhibitory concentrations ($IC_{50}$) of KGM, D-mannose, KGM-D-mannose and 5-FU and their inhibitory effects on HepG2 and WRL68 cell lines,
3. To analyse the expressions of apoptotic and proliferation associated genes in HepG2 and WRL68 cells post-treatment by real-time reverse transcription polymerase chain reaction (qRT-PCR) technique,
4. To differentiate liver cancer cell line HepG2 from normal liver cell line WRL68, and evaluate the post-treatment effect on HepG2 based on membrane dielectrical properties using DEP biosensor technique.

## 1.5 Dissertation Outline

The dissertation consists of 7 sections as follows:

1. Introduction. This chapter introduces the significant concern on the current hepatocellular carcinoma (HCC) occurrence worldwide and the challenges and limitations in diagnosis and treatment of HCC (research problems). It also further describes the outline, overall aim and specific objectives of this study.
2. Literature review. This chapter describes the relevant comprehension supporting the topics of interest. The content is based on the recent published works by accredited scholars and researchers that are directly related to the study. It provides crucial information on the theories, models, materials and techniques used in the research. Besides, it provides key understanding on the limitations of the previous works and potential improvements which had been improvised in the current research.
3. Methodology. This chapter describes the materials and equipment, as well as elaboration of methods used in the study, which includes the research design, procedures and statistical assessment of the collected data.
4. Results. The research findings are tabulated in tables and figures, along with complete descriptions.
5. Discussion. This chapter provides interpretation and discussion of the results. The findings from the current study are compared and supported with the discoveries from the previous works in the related fields. It also comprises of the strength and limitations of the current work.
6. Conclusion. This chapter summarises the research findings and their contributions in the current study as well as the future perspectives.
7. References. All supporting works or studies related to the current study are presented in the form of citations.

# CHAPTER 2

# LITERATURE REVIEW

Literature review describes the relevant comprehension supporting the topics of interest. The content is based on the recent published works by accredited scholars and researchers that are directly related to the study. It provides crucial information on the theories, models, materials and techniques used in the research. Besides, it provides key understanding on the limitations of the previous works and potential improvements which had been improvised in the current research.

## 2.1 Cancer

Cancer or malignancy is the complex genetic disease arises due to the abnormal cell growth or neoplasia in the body (Donaldson, 2004). Benign tumour is not cancerous as it does not metastasise, but overtime, this mass of cells can become malignant and invade the basement membrane of the local tissue and spread to other parts of the body. This might lead to death (Silva, 1999). Cancer cells developed due to the mutations in genes coding for regulatory proteins that give rise to the abnormal intracellular activities and disrupt the normal cell proliferation and functions. The cells lose the ability to repair the damaged DNA and continue to divide forming immortal daughter cells carrying faulty genetic materials (Prakash et al., 2013).

According to World Health Organisation (WHO) in 2014, cancer remains the fourth killer disease worldwide and ranked the sixth death causing disease in Malaysia.

Recently, Globocan 2012, estimated that the number of new cancer cases in 2012 is 14.1 million and it will keep increasing to 19.3 million per year by 2025 (International Agency for Research on Cancer, 2013). This online database also showed that the overall cancer incidence in Malaysia in 2014 is 37,426 cases per 100,000 and the number is expected to reach 79,441 in the next 5 years (International Agency for Research on Cancer, 2017).

Cancer cells are differed from the normal cells as they acquired a succession of six hallmark capabilities namely sustaining proliferative signalling, evading growth suppressors, resisting cell death, enabling replicative immortality, inducing angiogenesis, and activating invasion and metastasis as shown in Figure 2.1. Expressions of certain traits enable cancer cells to become tumourigenic and eventually malignant (Hanahan & Weinberg, 2011).

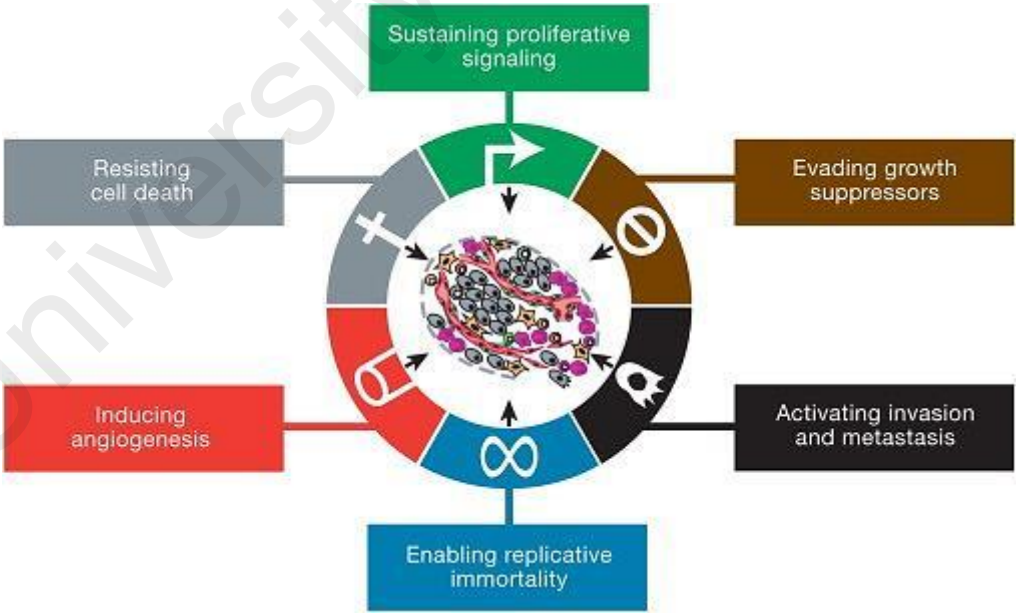


**Figure 2.1:** A model illustrated the basic hallmarks of cancer defining six properties a tumour acquires (Hanahan & Weinberg, 2011)

## 2.2 The Six Hallmarks of Cancer

### 2.2.1 Sustaining Proliferative Signalling

Homeostasis of cell number, maintenance of normal tissue architecture and function are carefully managed through control production and function of growth-promoting stimuli that aid in cell division and growth (Diederichs & Gutschner, 2012). Cancer cells however, acquire ability to constantly proliferate without external stimulation. Deregulation of cell growth signalling cascades disrupts the normal cell division cycle; stimulating uncontrolled downstream growth factors induced signalling pathways, which results in unlimited division (Hanahan & Weinberg, 2011).

The proliferation signals independency in cancer cells is achieved in several ways namely autocrine stimulation via self-producing growth factors and corresponding receptor molecules; paracrine signalling that stimulates growth factors production in normal or tumour-associated cells to support cancer cells growth; alterations in growth factor levels and receptor signalling cascades resulting in hyperresponsive cancer cells; as well as complete withdrawal from exogenous growth factors due to continuous activation of downstream signalling pathways and disruption of negative-feedback mechanisms (Diederichs & Gutschner, 2012). Often these signals influence cell cycle and cell growth, as well as cellular metabolism and viability (Hanahan & Weinberg, 2011).

### 2.2.2 Evading Growth Suppressors

Evasion of anti-growth signalling and loss of tumour suppressors' activities are highly complementary hallmarks in cancer cells to sustain the proliferative signalling. Loss of growth control mechanism is vital in neoplastic cells as it allows unlimited cellular

replication and circumvents elimination, cell cycle arrest and senescence by tumour suppressor proteins (Amin et al., 2015).

Several tumour suppressor genes (TSG) such as tumour protein p53 (Tp53), phosphatase and tensin homolog (Pten) or retinoblastoma protein (RB) had been discovered to regulate cell growth and proliferation. Activation of TSGs via external or internal stimuli results in cell cycle arrest, senescence and programmed cell death (Hanahan & Weinberg, 2011). Therefore, inactivation and repression of these genes are critical in carcinogenesis. It has been reported that over 70% of solid tumours underwent genetic changes mainly in TSGs which associated with the subsequent un-targetable cancer problems (Kohno & Yokota, 1999).

### 2.2.3 Resisting Cell Death

Apoptosis insensitivity has been a major strategy in malignancies which cells acquired in eliminating the cell death mechanisms, thus the development into high-grade malignancy and chemoresistance (Safa, 2016; Roberti, La Sala & Cinti, 2006). The notable apoptosis refractoriness in cancer cells includes imbalance signalling as a result of oncogene overexpression and genetic alterations associated with hyperproliferation (Adams & Cory, 2007).

Cancer cells evolve a several ways to attenuate or evade apoptosis. It usually involves the loss of function of p53 tumour suppressor proteins, which eliminates apoptosis-inducing stimulation. Alternatively, tumours disrupt the expressions of anti- and proapoptotic Bcl-2 family regulatory proteins by upregulating antiapoptotic regulators (Bcl-2, Bcl-xL) or the survival signals (Igf1/2), and downregulating proapoptotic factors

(Bax, Bim, Puma), generating high anti- to proapoptotic ratio and cell death resistance (Adams & Cory, 2007). Diverse apoptosis resistance approaches were developed throughout the evolution of cancer cell populations contributed to adverse malignancy status (Hanahan & Weinberg, 2011).

### 2.2.4 Enabling Replicative Immortality

Cellular senescence plays a notable role in tumour suppressive mechanism, leading to persistent cytostasis (inhibition of cell growth and proliferation). It is a robust inhibitory mechanism as cells will remain susceptible to senescence despite functional inactivation of one or more senescence pathway components (Yaswen et al., 2015). This is however, unlike normal cells which are only limited to specific successive cell growth-and-division cycles, neoplastic cells develop unlimited replicative ability in order to generate macroscopic tumours (Diederichs & Gutschner, 2012). Failure of senescence in cells is induced via multiple stimuli namely telomere dysfunction, oncogene activation, exogenous DNA damaging or oxidative agents resulting in changes favouring malignancy and drug resistance (Yaswen et al., 2015).

Telomeres or the chromosome ends are vital replication limit in cells in which shortening of telomeric DNA after each cell division controls the total division cycles (Multani & Chang, 2007; Counter et al., 1992). Tumour cells acquire major strategies to circumvent the loss of telomeres allowing replicative immortalisation. A specialised enzyme telomerase was found to be expressed in 90% of human malignancies. This enzyme adds the telomeric repeats to the chromosome ends enable the cells to resist telomere shortening (Shay & Wright, 2002).

### 2.2.5 Inducing Angiogenesis

Like normal tissues, tumours require nourishment in the form of nutrients and oxygen as well as the ability to eliminate metabolic wastes and carbon dioxide. Tumour angiogenesis generates the tumour-associated neovasculature, new blood vessel network that penetrates into tumourous growth to address the sustenance needs (Gupta & Qin, 2003). During tumourigenesis, an angiogenic switch is permanently activated; cancer cells secrete angiogenic growth factors such as vascular endothelial growth factor (VEGF) and basic fibroblast growth factor (bFGF) which interact with the surface receptors expressed on the endothelial cells and dictate angiogenesis (Sebti & Hamilton, 2000).

Overexpression of tumour-secreted angiogenic growth factor is insufficient to support angiogenesis, it usually occurs in complement with down-regulation of angiogenic negative regulators or inhibitors (Ziyad & Iruela-Arispe, 2011). Massive buildup of angiogenic growth factors at a vascularisation milieu causing neovasculature to develop into capillaries, mature venules or arterioles locally without further penetration into cancerous site. Most cancers evade this process by secreting angiogenic factors that mediate regression, inducing cell cycle arrest or apoptosis and switch the endothelial cells to angiogenic phenotype. Overtime, the angiogenic endothelial cells disrupt the local equilibrium between positive and negative regulators. High positive to negative regulators ratio stimulate the growth of invasive microvessels creating optimum environment favouring high-grade malignancy (Hoeben et al., 2004).

### 2.2.6 Activating Invasion and Metastasis

In epithelium-derived malignancies, maintaining a coherent primary tumour mass is vitally supported by inter-cellular structures and cell-cell adhesion (Jiang et al., 2015). Abnormalities in these structures in cancer cells via mutation or dysregulation alter the cell to cell and to extracellular matrix (ECM) attachments. These changes play a crucial role in detachment of the primary tumour and enhance dissemination and metastasis of cancer cells to secondary sites (Cavallaro & Christofori, 2004).

The most notable modification involved the loss E-cadherin in carcinoma cells. The loss of E-cadherin disrupts the cell to cell adhesions and concurrently disturbs the expression of cell cycle regulators $p27^{kip1}$ and $p57^{kip2}$, the proteins involved in inhibiting the cell to cell contact in normal epithelium (St Croix et al., 1998). E-cadherin aids to assemble epithelial cell sheets and form the adherent junctions between adjacent epithelial cells, allowing cells to remain inert within the sheets. It has been proven that up-regulation of E-cadherin antagonises the invasion and rapid metastasis in most cancers. On the contrary, mutational inactivation and reduced expression of E-cadherin in human carcinomas serve as a key suppressor of this hallmark capability (Berx & van Roy, 2009; Cavallaro & Christofori, 2004).

## 2.3 Hepatocellular Carcinoma

Hepatocellular carcinoma (HCC) is the primary liver cancer which covers approximately 90% of liver cancer cases and listed as the third most lethal neoplasms. HCC patients exhibit no symptoms at early stage and were usually detected at advanced stage which it is closely associated with decompensated cirrhosis, at which the available therapeutic options are limited and ineffective. Over the last 20 years, HCC was

uncommon in Western Europe, thus the disease provoked least attention among the scientific community. However, the occurrence rate of HCC significantly increases in the 21st century and is now the leading cause of death among patients with liver cirrhosis (Forner, et al., 2014).

The lack of awareness of the signs and symptoms of liver cancer, financial constrain to cover the costs of diagnosis and treatment in developing countries resulting in late diagnosis, and a higher mortality rate than in Western countries (Merriam & Muhamad, 2013). Furthermore, limited health infrastructure is another major problem in liver cancer control in Malaysia. As reported by Norsa'adah and Zayani (2013), many liver cancer cases were not diagnosed due to the lack of ultrasound, CT scan or liver biopsy facilities. These facilities are mostly accessible in general hospitals in Malaysia, while the invasive liver biopsy is highly unwelcome among the patients. Unlike developed countries, no screening programme is provided in Malaysian population which gives rise to late detection of liver cancer. In United States and Western Europe, American Association for the Study of Liver Diseases (AASLD) and European Association for the Study of the Liver (EASL) recommend screening and surveillance among high-risk patients by ultrasound every 6 months, aiming in detection of HCC at early stage, where the curative therapy are promisingly effective (Danila & Sporea, 2014).

### 2.3.1 Diagnosis of Hepatocellular Carcinoma

Current clinical screening of liver cancer includes both serological markers such as α-fetoprotein (AFP) and des-gamma-carboxy prothrombin (DCP) at 6-month interval, and radiological tests namely ultrasound, computerised tomography (CT) and magnetic resonance imaging (MRI) (Llovet, Fuster & Bruix, 2004).

Since 1980s, ultrasound scanning has been utilised to identify intrahepatic lesions (Takashima et al., 1982) in which its sensitivity is varied and highly operation and equipment dependent, ranging from 35 to 84% (Saar & Kellner-Weldon, 2008). Ultrasound is a highly specific HCC screening method with more than 90% specificity as reported by Bolondi et al. (2001) in their surveillance programme of cirrhotic patients for early diagnosis and treatment of HCC. This method nevertheless failed to detect 85% of lesions with ≤ 2 cm small HCC nodules (Achkar et al., 1998). Furthermore, patients with central obesity hinder the ability of ultrasound in small lesions detection (Brahee et al., 2013).

The limitations of ultrasound however are overcome with the introduction of advanced imaging technologies, CT scanning and MRI. CT and MRI has been found to be highly sensitive (90% sensitivity) in detecting ≥ 2 cm tumours. Sensitivity detection of tumours between 1 and 2 cm is 65% for CT and MRI at 80 to 92%, while tumours <1 cm is 10% and 34 to 71%, respectively (Colli et al., 2006). Despite high sensitivity, these two methods are not cost effective.

Serological marker AFP has long been used in HCC detection since the late 1960s (Wong, Cheung & Ahmed, 2014). One major disadvantage is that serological test of serum AFP is false positive as AFP levels can be highly expressed in patients with active hepatitis but no sign of HCC though its sensitivity and specificity are fairly high as reported by several surveillance studies (Di Bisceglie et al., 2005).

Most diagnostic approaches fail to sense abnormal liver cells until they become malignant and metastasise. Some test result parameters might overlap with other liver diseases which give a false positive diagnosis (Llovet, Fuster & Bruix, 2004). The

limitations in liver cancer diagnosis and the increasing in new incidence have gained broad interest among the researchers in the development of new diagnostic tools for detection of liver cancer at earlier stage, which effective treatments are feasible.

### 2.3.2 Treatment of Hepatocellular Carcinoma

Key advances in the treatment of HCC have been developed in the past two decades. There are multiple treatment options available including orthotopic liver transplantation (OLT), radiofrequency ablation, microwave ablation, trans-arterial chemoembolisation, percutaneous ethanol injection, radioembolisation and systemic chemotherapy (Lloviet, Fuster & Bruix, 2004). Treatment selection is highly dependent on tumour stages, underlying liver function and extrahepatic spread (Balogh et al., 2016).

Traditional chemotherapy remains the most common treatment option for most human cancers. Unfortunately, cancer cells tend to develop chemoresistance, which affect the effectiveness of the treatment. Wang, et al. (2010) reported that the chemoresistant HCC cell lines displayed cancer stem cells characteristics, such as self-renewal ability, multiple drug resistance, tumourigenicity and motility. Octamer 4 (Oct4) messenger RNA (mRNA) levels were significantly expressed in chemoresistant liver cancer cells due to DNA demethylation and enhance cells proliferation through apoptosis inhibition. Overtime, the cells alleviate the antiproliferative effects of drugs such as 5-fluorouracil (5-FU), doxorubicin and cisplatin.

Prevention of HCC is possible if appropriate measures are engaged. These include hepatitis B virus vaccination, introduction of antiviral therapy, regular full blood screen, and education on the effects of alcoholism and intravenous drugs. Constant improvements in surgical and nonsurgical approaches significantly increased the

survival benefits among HCC patients. Nonetheless, OLT remains the most effective surgical approach; the shortage of clinically complement organs impedes this therapy for most HCC patients (Balogh et al., 2016).

### 2.3.3 WRL68 Normal Liver Cell Line

American Type Culture Collection (ATCC) received the first human hepatic WRL68 cells culture in July, 1969. Mycoplasma contamination in the culture was detected and treated with antibiotic Ciprofloxacin. Epithelial WRL68 cell line is often used as a model of normal human liver cells in comparison studies as it displays similar morphological identities to hepatocytes and primary liver cell cultures. Secondary WRL68 cells have been proven to secrete several vital liver specific metabolites and enzymes namely albumin, α-fetoprotein, alanine amino transferase, aspartate amino transferase, gamma-glutamyl transpeptidase and alkaline phosphatase. WRL68 cell line was considered to be the derivative of human cervical cancer cell line HeLa. The standard polymerase chain reaction (PCR) DNA profiling shown indistinguishable features between two cell lines and both were found to contain Human Papilloma Viral (HPV) strain (American Type Culture Collection, 2016; Gutierrez-Ruiz et al., 1994).

### 2.3.4 HepG2 Liver Cancer Cell Line

HepG2 is a pure HCC cell line derived from the liver tissue of a 15 year-old male Caucasian. HepG2 is often used as an *in vitro* HCC model supported by the facts that it is epithelial in morphology, showed no evidence of Hepatitis B viral infection and expresses important hepatic enzymes such as 3-hydroxy-3-methylglutaryl-CoA reductase and hepatic triglyceride lipase which aid in cholesterol production and

triglyceride hydrolysis, respectively (American Type Culture Collection, 2016; Busch et al., 1990). High degree of morphological and functional differentiation *in vitro* of HepG2 makes it a compatible model in liver metabolism, xenobiotic toxicity, cytotoxic and genotoxic studies (Costantini, et al., 2013; Mersch-Sundermann et al., 2004).

## 2.4 Konjac Glucomannan

Konjac glucomannan (KGM), a water-soluble fibre derived from the tubers (Figure 2.2A) of *Amorphophallus konjac* K. Koch (Figure 2.2B), of Araceae family. This edible corm is commonly known as konjac or elephant yam native to tropical and subtropical eastern Asia (Fang & Wu, 2004). It is a straight chain polymer containing 1.6 to 1 ratio of β-1→4 D-mannose and D-glucose units with approximately 8% branching via β-1→6-glucosyl linkages (Shah et al., 2015) as shown in Figure 2.2C. Fresh raw konjac corm contains roughly 12% KGM while the purified konjac powder made up of nearly 97% KGM content with molecular weight of 666.579 g/mol (Fang & Wu, 2004). Glucomannan is viscous in water solution and non-digestible in the human small intestine (Katsuraya et al., 2003). The konjac flour was traditionally added in foods such as konjac jelly, tofu and noodles for over 2000 years, in which it was believed to aid in detoxification, tumour-suppression, and treatments for respiratory diseases as well as skin disorders. Until recently in the past two decades, the purified konjac flour had been introduced in the United States and Europe as food additive and a dietary supplement for weight loss, blood sugar and cholesterol control (Chua et al., 2010).

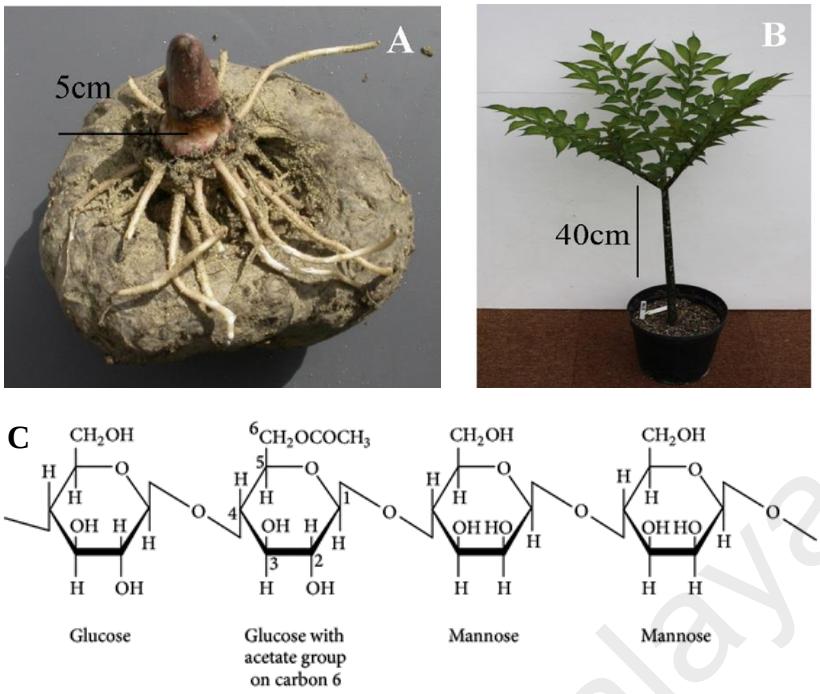


**Figure 2.2:** *Amorphophallus konjac* K. Koch, (A) konjac corm; (B) konjac plant; (C) chemical structure of konjac glucomannan (Shah et al., 2015)

## 2.5 Therapeutic Properties of Konjac Glucomannan

### 2.5.1 Prebiotic and Antioxidant Activities

A time-course study by Wu, Cheng & Chen (2011) determined the effect of KGM on human faecal β-glucuronidase activity, secondary bile acid levels and faecal water toxicity towards human colonocytes model, Caco-2 cells. Faecal β-glucuronidase activity significantly lessened by 31.5% along with 10.5% increment of faecal β-glucosidase activity, but faecal β-galactosidase activity remains unchanged in KGM-supplemented individuals. The results suggested that daily supplementation of KGM as low as 4.5 g/day was sufficient to reduce bacterial β-glucuronidase in the human colon and minimised toxin formation. Reduction in β-glucuronidase activity may be the result of decreased clostridia population that potentially produces larger amount of β-glucuronidase than lactobacteria or bifidobacteria. KGM consumption is therefore shown to moderate the β-glucuronidase-mediated toxins formation in colon (Klinder et al., 2004).

The same study further reported the significant reduction of human faecal water cytotoxicity towards Caco-2 cells in KGM-supplemented diet. The greater cytoprotective effect of KGM is closely related to its fermentation end product, butyrate, which serves as a key energy source for colonocytes and scavenging the free radicals, protecting the colon mucosal linings (Canani et al., 2011). Furthermore, KGM lowered the production of secondary bile acids, tight junctions-damaging metabolites in colon, resulting in further reduction of cytotoxic effect of faecal water towards Caco-2 cells (Commane et al., 2005).

The protective antioxidant activity of KGM against oxidative stress was further assessed via co-incubation of Caco-2 cells in faecal water and hydrogen peroxide ($H_2O_2$) combination. The defensive capacity of KGM-supplemented faecal water against oxidative $H_2O_2$ significantly higher than the placebo faecal water, suggesting the free-radical-scavenging ability is mediated by fermentation of KGM by lactic acid bacteria. The results conclude that daily KGM consumption improved the faecal microbial ecology and metabolites, providing a promising cytoprotective role of faecal water which reduces the precancerous risk factors in human colon (Wu, Cheng & Chen, 2011).

In another study by Wu & Chen (2011) further supports the antioxidant activity of KGM, in which the incorporation of this fibre in high-fat fibre-free diet rats significantly reduced the DNA damage via enhancing the expression of genes encode for antioxidant enzymes glutathione peroxidase, superoxide dismutase and catalase in colonic mucosa and liver. Moreover, KGM provides systemic antioxidative activity in rats by stimulating α-tocopherol production, a free-radical scavenging vitamin E in blood. In short, the roles of KGM in colonic ecology control and antioxidative defence

activities supported its traditionally known potential anti-cancer properties, which, indeed merits further exploration.

### 2.5.2 Anti-obesity Activity

The potential approach of KGM in controlling the blood cholesterol and glucose levels widely promoted it as a dietary supplement used for weight loss (Keithley et al., 2013). The viscous, low energy density and bulking natures of KGM prolongs the gastric emptying time, boosts satiation by displacing the energy of other nutrients as it absorbs water and expands in the gastrointestinal tract, which long-term ingestion decreases the desire of consuming food high in cholesterol and glucose concentrations, reduces body fat mass (Sood, Baker & Coleman, 2008; Doi, 1995).

Furthermore, a study by Gallaher et al. (2000) reported that rat model fed with daily 10 g/100 g of KGM reduces the total liver cholesterol level by 42% indicated suppression of hepatic cholesterol synthesis along with 18.2% reduction in intestinal cholesterol absorption due to increased viscosity, which increases the faecal elimination of cholesterol containing bile acids (Chearskul, Kriengsinyos & Kooptiwut, 2009; Chen et al., 2003). Rats tested with addition of KGM in high-cholesterol diet were shown to have lower weight gain as compared to the control group (Gallaher et al., 2000).

### 2.5.3 Laxative Effect

KGM is safe to be taken by children, pregnant women and healthy individuals to ease the bowel movement and relieve constipation. Increased stool bulk and improved colonic ecology has shown to be associated with the laxative effect of KGM (Chen et

al., 2006). Baucke et al., (2004) found that glucomannan is effectual in treating constipation in children without any significant side effects such as abdominal discomfort, excessive gas and bloating, diarrhoea or allergic reactions.

Another study reported 1 to 3 months consumption of glucomannan with daily intake of 1.45 g in constipated pregnant women promoted a return to normal frequency of weekly evacuations by 4.9 to 5.8 times/week (Signorelli, Croce & Dede, 1996). In addition, 4.5 g/day of KGM supplementation in low-fibre diets increased the bowel movement frequency up to 30% and improved colonic microbiota in slightly constipated adults (Chen et al., 2008).

The ability of KGM to retain water in gut further induced its laxative nature. Constipated rats administered with KGM in the diet showed significant increment in water content and weight of faecal pellet with improved intestinal motility. High glucomannan content in KGM enables it to absorb water approximately 138 to 200% in the gut, promoting smoother bowel evacuation (Widjanarko, Wijayanti & Sutrisno, 2013).

## 2.6 DEP Biosensor Technique

### 2.6.1 Historical Background

For over five decades of multiple researches, dielectrophoresis (DEP) separation technique had improved greatly. The concept of electrophysiological separation was first described in 1923 by Hatschek and Thorne but not until 1966 that it was notably termed as dielectrophoresis (Hughes, 2016). It was first effectively applied to biological cells by Pohl and Hawk in 1966 to electrically characterise and separate the live from

the dead yeast cells. The apparatus setup was simple, made up of a pair of electrodes, one a plate and the other a needle, forming a "point and plane" arrangement which later connected to a signal generator. A solution containing live and dead yeast cells was tested using the device which the live cells immediately attracted to the electrodes upon application of 2.55 MHz signal at 30 Vrms. Despite the effective separation, attachment of cells to the electrodes remained a major drawback as this restricted electrode reusability (Hughes, 2016: Pohl & Hawk, 1966).

DEP in a lab-on-a-chip (LOC) device was later developed by Masuda and coworkers in 1989 based on "fluid integrated circuit" concept. Two micropumps containing distinct cell types propelled the cells into dielectrophoretic chamber, forming cells pearl-chain. A constant pulse voltage was applied, drawing the dielectric fusion of phenotypically similar cells which was then collected at a specific cell-fusion electrode. This device combined small dimension cell-handling components into a miniaturised device which enabled automated single cell separation under a specific pulse voltage without any notable cell-to-electrode adhesion problems (Yafouz, Kadri & Ibrahim, 2013; Masuda, Washizu & Nanda, 1989).

### 2.6.2 Principle of DEP Biosensor

The concept of DEP is that any polarisable particles suspended in a similarly polarisable medium can be made to move when applied to a non-uniform electric field (Nastruzzi et al., 2007). According to Mulhall et al. (2011), the direction of the particle's motion depends on the difference between the polarisability of the particle and the medium. The movement of particles towards the high field strength regions of the electrode indicates higher polarisability of the particle than the medium. This phenomenon is known as

positive DEP (+DEP, p-DEP). On the other hand, negative DEP (−DEP, n-DEP) force is generated when the suspending medium is more polarisable than the particle; pushes the particles away and accumulate at the low field strength regions of the electrode. Furthermore, when there is a net balance in polarisability of the particle and the medium, the force of attraction and repulsion from the high field strength regions will cancel each other and the particle will remain static known as crossover frequency.

DEP force is derived based on the permittivity, the ability to store electrical energy in an electric field, and conductivity of both suspended medium and biological cells. The permittivity and conductivity differ in different cell lines as each has a distinctive thickness and characteristics of plasma membrane. These unique features of cells are varied in normal and diseased states for example the membrane of cancerous cells contains higher number of folding, irregular bulges, disarrangement and microvilli which is highly distinguishable from the normal cells. Such changes in cancerous cells are potentially affecting the membrane electrical property even at the slightest degree and simultaneously altering the DEP forces of cells at different stages of cancer (Mulhall et al., 2011; Pethig & Khell, 1987).

### 2.6.3 Design and Operation of DEP Biosensor

The device was made up of 5 layers, consisting of top and bottom layers, and a microelectrode, a spacer and an indium tin oxide (ITO) layer sandwiched in between, as shown in Figure 2.3(a). The gold microelectrode fabrication was carried out using standard photolithography method, a series of steps that uses light treatment to coat the preferable geometric pattern on a transparent solid surface such as glass slide and assumed the shape of complete fabrication as in Figure 2.3(b). There are 16 dots that

served as the channel for the particles. Individual dot has an inner diameter of 200 µm and an outer diameter of 300 µm. The 16 dots are clustered into 4 groups of four dots with each group has the capability to be simultaneously energised with different signal frequencies. The spacer is a microfluidic gasket that contains microchannel for capillary fluid flow. ITO glass slide acts as the counter electrode which its transparency is best suited for microscopic monitoring of cells during DEP experiments compared with opaque electrodes (Yafouz, Kadri & Ibrahim, 2014).

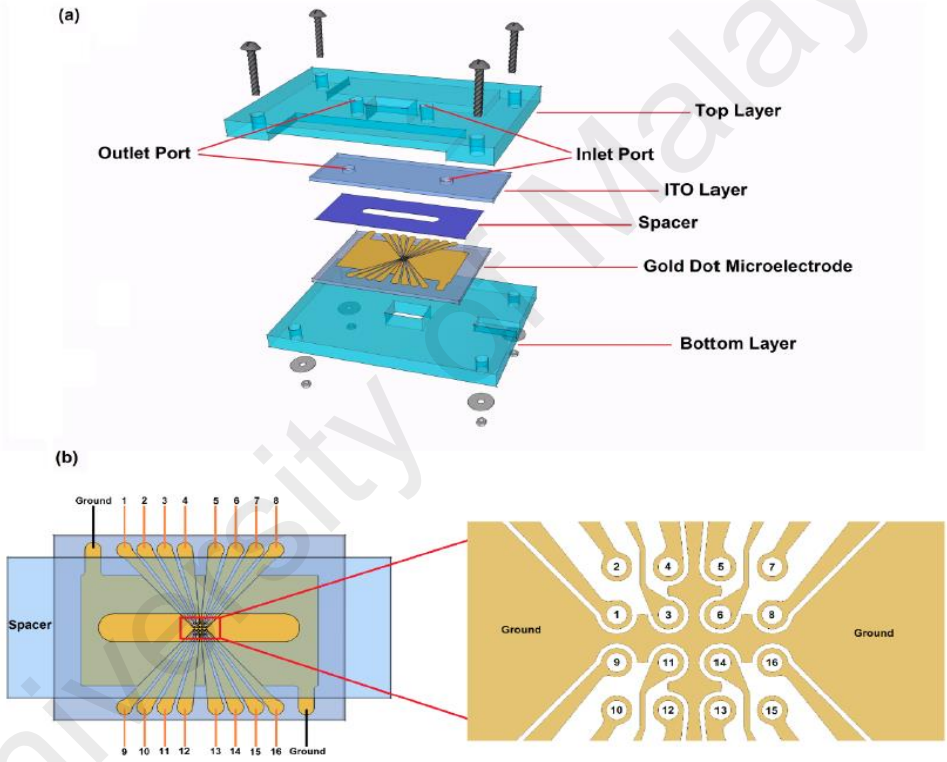


**Figure 2.3:** DEP biosensor design (Yafouz, Kadri & Ibrahim, 2014)

Hollow-centred circular geometry of the DEP microlectrodes enables light to pass through and ease the microscopic observation of cells' motion. The light intensity shift in the central region of the dot is then calculated based on the cells movement and generated a "DEP spectrum", reflecting the DEP forces experienced by the cells as illustrated in Figure 2.4. The phenomenon in which cells homogenously distributed over

the dot area (Figure 2.4(1)) is known as reference state or no DEP effect. However, cells move away from the dot centre and accumulated at the high electric field region of the microelectrode or dot edge as shown in Figure 2.4(2) indicates positive DEP (p-DEP) force. Figure 2.4(3) illustrated the opposite effect which the negative DEP (n-DEP) force draws the cells movement towards the low electric field central region of the dot (Yafouz et al., 2016).

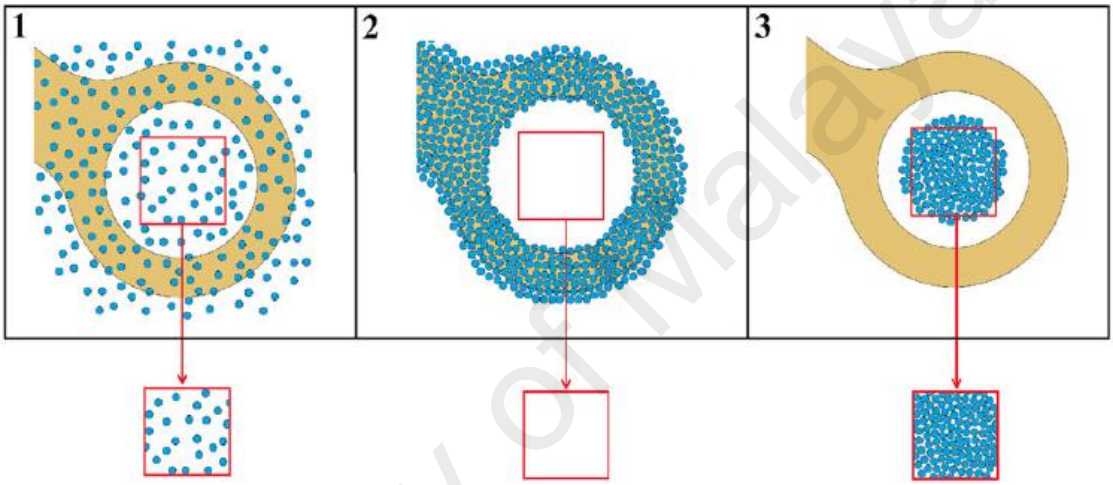


**Figure 2.4:** The operation principle of DEP biosensor dot electrodes (Yafouz et al., 2016).

## 2.7 Applications of DEP Biosensor

### 2.7.1 Isolation of Cancer Cells

Over the past three decades, DEP plays a major role in cell separation and characterisation. The DEP technique has been greatly utilised in biomedical applications especially separation of selective target cells, three-dimensional cells manipulation, advanced biological molecular screening and biosensors (Demircan, Ozgur & Kulah, 2013). Non-invasiveness, high selectivity and low cost DEP technique provides a promising trend towards point-of-care (POC) systems. The ability of DEP in cells characterisation solely via dielectric properties of bioparticles without the need of

specific tags or chemical reactions remains one of the major advantages of DEP in biomedical research including cancer and chronic diseases studies (Yafouz, Kadri & Ibrahim, 2012).

One of the earliest DEP separations in cancer studies was conducted by Gascoyne and his team at University of Texas in 1997. The study aimed in separating the breast cancer MDA-231 cells from blood effectively retained MDA-231 cells by the DEP electrodes while blood cells were eluted along with the eluate at 80 kHz signal frequency (Gascoyne et al., 1997).

A study by Antfolk et al. (2017) integrated DEP in an electroactive microwell array (EMA) for single-cell isolation of prostate cancer cells (DU145) from the peripheral blood mononuclear cell (PBMC) fraction. The target cells were pre-aligned and separated from the unwanted cells before entering the EMA chip. The isolated target cells were concentrated and collected at specific DEP-mediated microwells in EMA chip based on respective dielectric properties. At a constant signal frequency of 5 MHz at electrical potential of 10.7 V, 71% of DU145 cells were isolated and recovered in DEP microwells with the PBMC contamination rate as low as 0.03%. DEP-integrated EMA is highly applicable for label-free direct separation and identification of cancer cells in single-cell format as it effectively eliminated sample loss occurrence and contamination rate (Antfolk et al., 2017).

### 2.7.2 *In vitro* Liver-cell-on-chip Patterning

A team of researchers from National Tsing Hua University of Taiwan applied an enhanced field-induced dielectrophoresis trap technology in reconstruction of hepatic

lobular radial pattern on-chip mimicking the real liver tissue. This study aimed to recreate the liver lobular pattern *in vitro* which provides non-invasive alternative in liver tissue histology (Ho et al., 2006).

The concentric-stellate-tip DEP electrode was designed to dielectrically manipulate the live hepatocytes and generate the lobule-mimetic radial pattern. Enhanced DEP trap allows spatial separation and distribution, and rapid patterning of hepatic cells according to the specific electric-field gradients, forming the desired biomimetic patterns on the microfluidic chip (Ho et al., 2006). This technology was further assessed for the compatibility in maintaining the viability of cells on-chip. Hepatocytes HepG2 and endothelial cells were first dielectrically patterned on the microfluidic chip. Fluorescent assay was then conducted on the cells and it showed that 95% of the cells remain viable after patterning (Ho et al., 2013).

### 2.7.3 Discriminating Dengue-infected Hepatic Cells

Yafouz et al. (2016) conducted a study to discriminate dengue-infected hepatic cells, WRL68 from the non-infected based on their crossover frequency detected by DEP device. Crossover frequency is the frequency which the net balance of n-DEP and p-DEP forces causing the cells to remain stagnant. A microarray dot electrode was used to conduct the DEP experiments. The results showed that the crossover frequency of dengue-infected normal liver WRL68 cells significantly decreased by approximately 36% from 220 kHz in the healthy counterparts to 140 kHz. This concludes the ability of DEP in direct characterisation of pre- and post-infection in cells solely via cells electrophysiological status (Yafouz et al., 2016).

With the above applications of DEP biosensor technique, this tool shown a potential POC system for discriminating normal and cancer liver cells at earlier stage of liver cancer as well as validating the post-treatment effects of anti-cancer agents; which in turn will help reduce the lethal liver cancer incidence and improve the survival rate among liver cancer patients. In this study, along with the traditionally known tumour suppression ability of KGM, DEP serves as a useful tool in determining the post-KGM treatment dielectric changes in HepG2 cells to further validate and be the first to assess the anti-cancer entity of natural product using DEP technique.

# CHAPTER 3

# METHODOLOGY

This chapter describes the materials and equipment, as well as elaboration of methods used in the study. It includes the research design, clear procedures adopted and statistical assessment of the collected data which provide the readers with clear description on how the data was obtained and generation of the research findings.

## 3.1 Materials

### 3.1.1 Cancer Cell Lines

Human hepatic cell line (WRL68, ATCC® CL-48™) and hepatocellular carcinoma cell line (HepG2, ATCC® HB-8065™) were used in this study. Both cell lines were obtained from American Type Culture Collection (ATCC) and cultured in recommended cell culture medium and protocol. Confluency of culture, cells morphology and contamination in cell culture medium were monitored daily using phase contrast inverted microscope (Nikon ECLIPSE Ti-S).

### 3.1.2 Chemicals and Solvents

The list of chemicals and solvents used in this study are shown in Table 3.1.

**Table 3.1:** List of chemicals and solvents

| **Chemicals/ Solvents** | **Manufacturer** |
|---|---|
| 5-flurouracil (5-FU) | Sigma-Aldrich, USA |
| Accutase | Nacalai Tesque Inc., Japan |
| Annexin V-FITC apoptosis detection kit I | Becton Dickinson, USA |
| D-mannitol | Sigma-Aldrich, USA |
| D-mannose | Merck & Co., Germany |
| Dulbecco's modified eagle medium (DMEM), low glucose | Nacalai Tesque Inc., Japan |
| Foetal bovine serum (FBS) | Capricorn Scientific, Germany |
| Isopropanol | Nacalai Tesque Inc,, Japan |
| Konjac glucomannan (KGM) | Health Plus, UK |
| 3-(4,5-dimethylthiazol-2-yl)-2,5-diphenyltetrazolium bromide (MTT) reagent | Sigma-Aldrich, USA |
| Phosphate-buffered saline, tablet (PBS) | Sigma-Aldrich, USA |
| Potassium chloride (KCl) | Sigma-Aldrich, USA |
| QuantiNova reverse transcription kit | Qiagen, Germany |
| RNeasy mini kit | Qiagen, Germany |
| SensiFAST SYBR Hi-Rox kit | Bioline, UK |
| Tryphan Blue stain 0.4% | Thermo Fisher Scientific, USA |
| Trypsin-EDTA solution | Nacalai Tesque Inc,, Japan |

### 3.1.3 Equipment

The list of equipment used throughout the study is shown in Table 3.2.

**Table 3.2:** List of equipment

| **Equipment** | **Manufacturer** |
|---|---|
| Autoclave ES-315 | TOMY Digital Biology, Japan |
| BD Accuri™ C6 Plus flow cytometer | Becton Dickinson, USA |
| Carbon dioxide ($CO_2$) incubator | Heraeus, Germany |
| Centrifuge | Thermo Fisher Scientific, USA |
| DDS function generator | GW Instek, Taiwan |
| Electronic balance | Mettler Toledo, USA |
| Freezer (-20$^0$ C) | National, Japan |
| Laminar flow tissue culture hood | Heraeus, Germany |
| Liquid Nitrogen tank | Chart Industries, USA |
| Microcentrifuge | Thermo Fisher Scientific, USA |
| NanoDrop-2000 spectrophotometer | Thermo Fisher Scientific, USA |
| Phase contrast inverted microscope | Nikon Instruments Inc., USA |
| Refrigerator (2-8$^0$ C) | National, Japan |
| StepOnePlus Real-Time PCR system | Thermo Fisher Scientific, USA |
| Tecan Infinite M1000 Pro microplate reader | Tecan Trading AG, Switzerland |
| Thermal cycler | Biometra, Germany |
| Vortex | Thermo Fisher Scientific, USA |
| Water bath | Memmert GmBH + Co. KG, Germany |

## 3.2 Methodology

The experimental design of the study is shown in Figure 3.1.

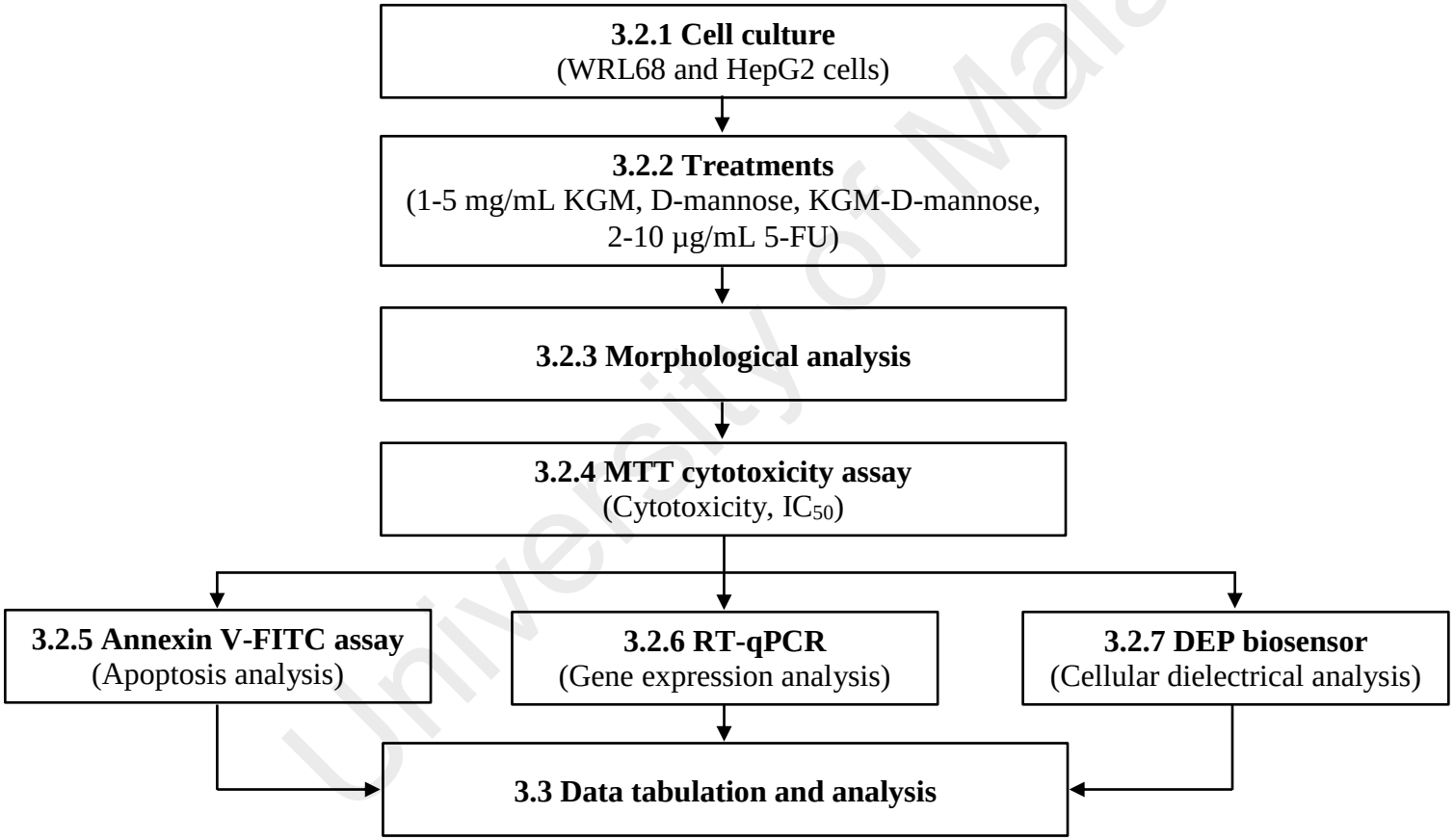


**Figure 3.1:** Research workflow

### 3.2.1 Cell Culture

All cell culture works were conducted under strict aseptic condition in a laminar flow tissue culture hood and followed standard cell culture protocol by American Type Culture Collection (ATCC). The complete growth medium (CGM) for cell culture was freshly prepared in which Dulbecco's modified Eagle's medium (DMEM) was mixed with heat-inactivated 10% foetal bovine serum (FBS) in 10:1 ratio. Vials containing human normal liver (WRL68) and liver cancer (HepG2) cell lines were thawed immediately by gentle agitation in the water bath at 37°C for one minute. The vials were then removed from the water bath and decontaminated with 70% ethanol. The thawed cryopreserved cell suspension (1 mL) were transferred to a sterile centrifuge tube containing 4 mL of DMEM and centrifuged at 1,500 rpm for 10 minutes to remove the cryoprotectant agent dimethyl sulfoxide (DMSO). Supernatant was discarded and the cell pellet was then resuspended in 1 mL CGM. The cell suspension was transferred to a sterile 25 $cm^2$ culture flask containing 4 mL CGM and incubated in 5% carbon dioxide ($CO_2$) incubator at 37°C. Cell confluency, morphology and culture media conditions were monitored daily by observing under the phase contrast inverted microscope.

#### 3.2.1.1 Subculture of Cell Lines

Subculture was performed upon 70 to 80% cell confluency. WRL68 and HepG2 cells are monolayers in culture, thus trypsinisation step is crucial. The old cell culture medium was removed and rinsed twice with 5 mL phosphate buffer saline (PBS), followed by addition of 1 mL of trypsin-EDTA solution. The cells were further incubated for 5 to 10 minutes for cell detachment. Approximately 4 mL of CGM was added once the cells detached completely to deactivate the activity of trypsin. The total

suspension was then centrifuged at 1,500 rpm for 10 minutes. The supernatant was removed and the pellet was resuspended with 2 mL CGM. The cell suspension was then equally divided into new culture flasks containing 4 mL of CGM and continues cultured in standard culture conditions.

### 3.2.1.2 Tryphan Blue Exclusion Assay using Haemocytometer

Cell suspension was prepared and into a sterile microcentrifuge tube, 100 µL of cell suspension was transferred and mixed with equal volume of 0.4% tryphan blue dye. Approximately 20 µL of the mixture was loaded to the haemocytometer and observed under phase contrast inverted microscope at 10× magnifications. The number of viable cells (unstained cells) in the four counting grids of haemocytometer was calculated using cell counter. The cell concentration was calculated via the formula in Equation 1,

$$\text{Cell concentration (cells/mL)} = \text{average cell count per square} \times DF \times 10^4 \times \text{volume of cell suspension} \quad (1)$$

In which,

DF = Dilution factor, 2 (2:1 dilution with tryphan blue)

$10^4$ = conversion factor converting $10^{-4}$ mL to 1 mL (refer **Appendix C**, Arrangement and dimensions of haemocytometer)

### 3.2.2 Preparation of Sample Solutions for Bioassays and DEP Analysis

In morphological evaluation and cytotoxicity assay (MTT), konjac glucomannan (KGM), D-mannose and KGM-D-mannose combination were prepared with concentrations ranging from 1 to 5 mg/mL, diluted from the initial stock of 10 mg/mL, as shown in Table 3.3. Standard chemotherapeutic drug, 5-FU, was used as the positive control in this study with concentrations of 2 to 10 µg/mL, with initial stock of 20 µg/mL (Table 3.4).

**Table 3.3:** KGM, D-mannose, KGM-D-mannose samples preparation

| Volume of initial stock (mL) | Volume of diluent CGM (mL) | Final volume (mL) | Final concentration (mg/mL) |
|---|---|---|---|
| 0.1 | 0.9 | 1.0 | 1.0 |
| 0.2 | 0.8 | 1.0 | 2.0 |
| 0.3 | 0.7 | 1.0 | 3.0 |
| 0.4 | 0.6 | 1.0 | 4.0 |
| 0.5 | 0.5 | 1.0 | 5.0 |

**Table 3.4:** 5-FU samples preparation

| Volume of initial stock (mL) | Volume of diluent CGM (mL) | Final volume (mL) | Final concentration (µg/mL) |
|---|---|---|---|
| 0.1 | 0.9 | 1.0 | 2.0 |
| 0.2 | 0.8 | 1.0 | 4.0 |
| 0.3 | 0.7 | 1.0 | 6.0 |
| 0.4 | 0.6 | 1.0 | 8.0 |
| 0.5 | 0.5 | 1.0 | 10.0 |

For apoptosis assay, gene expression and DEP analyses, half maximal inhibitory concentration ($IC_{50}$) of each treatment obtained from the graph of percentage of cell viability against concentration was used to treat WRL68 and HepG2 cells. The stock solutions were prepared to the final volume of 2 mL according to Table 3.5.

**Table 3.5:** Stock solutions ($IC_{50}$) preparation

| **Treatment** | **Dry weight of treatment (mg)** | **Volume of diluent CGM (mL)** | **Final concentration** |
|---|---|---|---|
| KGM | 7.2 | 2.0 | 3.60 mg/mL |
| D-mannose | 13.9 | 2.0 | 6.95 mg/mL |
| KGM-D-mannose | 14.5 | 2.0 | 7.25 mg/mL |
| 5-FU | 8.0 | 2.0 | 4.00 µg/mL |

### 3.2.3 Morphological Analysis

Approximately $1 \times 10^4$ of HepG2 and WRL68 cells were seeded in 12-well plate and incubated at 37°C in 5% $CO_2$ incubator for 24 hours. The cells were then treated with all concentrations of KGM, D-mannose, KGM-D-mannose and 5-FU as prepared in Section 3.2.2 and further incubated for 24 hours. The post-treatment morphological changes were observed and the images were captured using Nikon ECLIPSE Ti-S inverted microscope (Nikon Instruments Inc., New York, USA) at 24, 48 and 72 hours.

### 3.2.4 MTT Cytotoxicity Assay

Cytotoxicity evaluation using MTT assay was adapted from the protocol described by Van Meerloo et al. (2011). HepG2 and WRL68 cells were plated at $1 \times 10^3$ cells (100 µL per well) except sterility wells and incubated for 6 to 24 hours at 37°C in 5% $CO_2$ incubator. MTT assay was carried out in three 96-well plates. The cells were then treated with 50 µL of different concentrations ranging from 1-5 mg/mL of KGM, D-mannose, KGM-D-mannose, 2-10 µg/mL 5-FU as positive control and further incubated for 24, 48 and 72 hours, respectively. The basic culture medium DMEM was used as the negative control. Into sterility wells labelled "SC", 150 µL of CGM was added to ensure that the medium used for cell culture are sterile. Wells labelled "GC" were growth control standards to monitor the normal cellular growth and proliferation of cells used throughout the assay. The overall plate design for MTT assay is as illustrated in Figure 3.2.

After incubation, 10 µL 3-(4,5-dimethylthiazol-2-yl)-2.5-diphenyltetrazolium bromide (MTT) reagent was added and further incubated for 2 to 4 hours in dark until purple precipitate was visible. After incubation, 150 µL of growth medium was removed followed by addition of 100 µL isopropanol and mixed well. The absorbance was read immediately at 570 nm using Tecan Infinite M1000 Pro microplate reader. The percentage of cell viability was calculated for all treatments using the formula in Equation 2,

$$\text{Percentage of cell viability} = (A_{sample} / A_{NC}) \times 100\% \quad (2)$$

Where,

$A_{sample}$ = average absorbance of sample

$A_{NC}$ = average absorbance of negative control

The graphs of percentage of cell viability against concentration of drugs/compounds were plotted. Half maximal inhibitory concentration ($IC_{50}$) of each treatment was obtained from the graph.

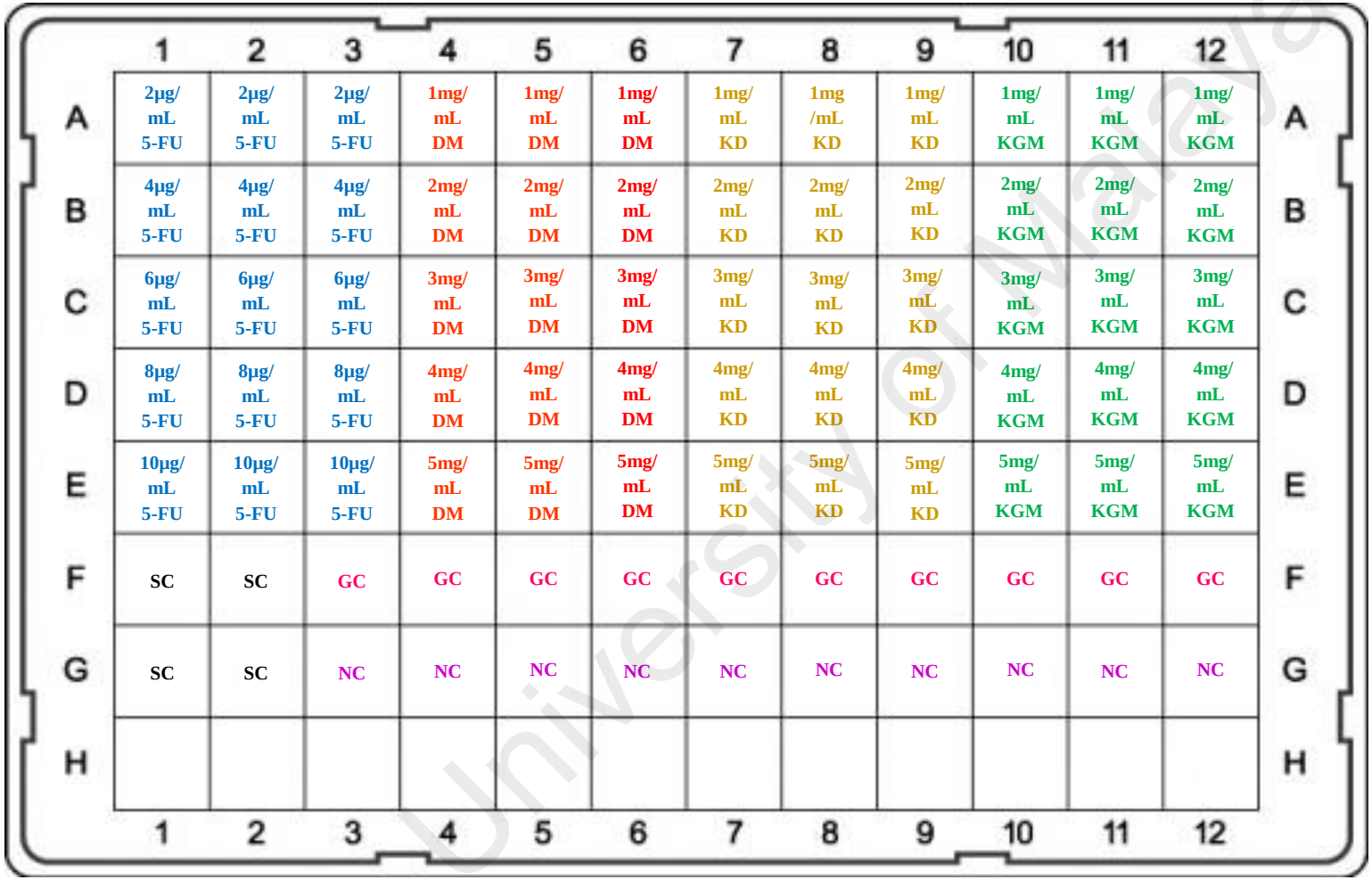


**Keys:**

**5-FU**, 5-fluorouracil (Positive control)

**DM**, D-mannose

**KGM**, konjac glucomannan

**KD**, KGM-D-mannose

**SC**, sterility control

**GC**, growth control

**NC**, negative control

**Figure 3.2:** Design of 96-well microtiter plate used in MTT assay

### 3.2.5 Annexin V-FITC Apoptosis Assay

Approximately $1 \times 10^6$ cells per well was plated in 12-well plate and incubated for 24 hours. KGM, D-mannose, KGM-D-mannose and 5-FU at $IC_{50}$ concentrations were used to treat WRL68 and HepG2 cell lines, 2 mL each, and further incubated for 24 hours. Untreated cells were used as the negative control in this assay in which 2 mL of CGM without any drug/compound was added to negative control well.

After 24 hours treatment, cells were detached using 1 mL accutase per well and washed twice with 1 mL cold PBS by centrifugation at 1,500 rpm for 10 minutes. Cells were further resuspended in 100 µL of 1× Binding Buffer provided in Annexin V-FITC apoptosis detection kit I and transferred to a 5 mL culture tube and mixed with FITC Annexin V and propidium iodide (PI), 5 µL each. The mixture was incubated for 15 minutes at room temperature in the dark and analysed using BD Accuri™ C6 Plus flow cytometer. These steps were repeated in triplicate for each cell lines.

The percentage of apoptotic events (non-apoptosis, early apoptosis and late apoptosis) in WRL68 and HepG2 cells after treatments was obtained directly from dot plots in BD Accuri™ C6 software. The triplicate readings of each apoptotic events were averaged and presented in stacked columns of percentage of cells against treatments for both cell lines.

### 3.2.6 Gene Expression Analysis

The real-time reverse transcription polymerase chain reaction (RT-qPCR) is the PCR-based technique to analyse the expression of gene of interests via quantification of template messenger ribonucleic acid (mRNA). The steps include (i) RNA extraction and

purification, (ii) reverse transcription of RNA template, (iii) real-time polymerase chain reaction (Nolan, Hands & Bustin, 2006).

### 3.2.6.1 RNA Extraction and Purification

HepG2 and WRL68 cells ($1 \times 10^6$ cells) were seeded in 12-well plate and incubated in 5% $CO_2$ incubator for 24 hours. Treatment group includes KGM, D-mannose, KGM-D-mannose and 5-FU at $IC_{50}$ concentrations in 2 mL CGM was added to the cells and further incubated for 24 hours. CGM was used as the negative control (untreated cells). The RNAs of treated and untreated cells were extracted and purified after treatments. These steps were done using RNeasy® Mini kit.

Treated and untreated HepG2 and WRL68 cells were lysed using 350 µL of lysis Buffer RLT, followed by equal volume of 70% ethanol and mixed well. Total of 700 µL cell lysate was transferred to an RNeasy Mini spin column (placed in a 2 mL collection tube) and centrifuged at 10,000 ×g for 15 seconds. The flow-through was discarded and 700 µL Buffer RW1 was added, spun at 10,000 ×g for 15 seconds. Same steps were repeated with 500 µL Buffer RPE, twice at 15 seconds and 2 minutes, respectively. The spin column was then transferred into a new 2 mL collection tube and 30 µL of RNase-free water was added directly to the spun column membrane. The RNA was eluted by centrifugation at 10,000 ×g for 1 minute.

The purity of the extracted RNAs was analysed using NanoDrop-2000 spectrophotometer. One drop of extracted RNA was loaded onto the lower measurement pedestal. The sampling arm was lowered and spectral measurement was initiated to measure the RNA purity and total RNA concentration (in nanogram per 1 µL, ng/µL)

using NanoDrop software. The purified RNA stocks were kept in the -20°C freezer for gene expression analysis.

### 3.2.6.2 Reverse Transcription

The extracted RNA (DNA synthesis template) was reverse transcribed to obtain complimentary DNA (cDNA) using QuantiNova Reverse Transcription kit. First, template RNA, genomic DNA (gDNA) Removal Mix and Reverse Transcriptase Enzyme were thawed on ice, while Reverse Transcription Mix and RNase free water at room temperature. The gDNA removal reaction mixture was prepared by mixing 2 µL of gDNA Removal Mix with 5 µg template RNA and RNase free water to the final volume of 15 µL. The mixture was then incubated at 45°C for 2 minutes and placed immediately on ice after incubation.

Reverse-transcription Master Mix was prepared on ice by adding 1 µL Reverse Transcriptase Enzyme into 4 µL Reverse Transcription Mix. The freshly prepared Reverse-transcription Master Mix was then mixed well with 15 µL gDNA reaction mixture, made up 20 µL of Reverse-transcription reaction mixture and proceeded to reverse transcription process. Reverse transcription was done using thermal cycler with fixed temperatures for cDNA synthesis: annealing step (25°C for 3 minutes), reverse-transcription step (45°C for 10 minutes) and inactivation of Reverse Transcriptase enzyme (85°C for 5 minutes). The cDNA stocks were kept in -20°C freezer for real-time polymerase chain reaction (qPCR).

### 3.2.6.3 Real-Time Polymerase Chain Reaction

The genes of interest are anti-apoptotic gene (BCL2, accession number NC_000018.10), pro-apoptotic gene (BAX, accession number NC_000019.10), tumour suppressor gene (p53, accession number NC_000017.11), cell cycle inhibitory gene (p16, accession number NC_000009.12) and proliferative gene (Cyclin D1, accession number NC_000011.10). The specific primer sequence of each gene was designed using Primer 3 software based on the published GenBank database sequences.

The genes of interest were analysed using SensiFAST SYBR Hi-Rox kit. SensiFAST SYBR® Hi-ROX Mix, forward and reverse primers of genes of interest and template cDNA from Section 3.2.6.2 were thawed on ice. PCR mastermix (final volume of 20 µL) was prepared by mixing 10 µL SensiFAST SYBR® Hi-ROX Mix, 0.8 µL of 10 µM forward primer, 0.8 µL of 10 µM reverse primer, 1 µL of cDNA template and 7.4 µL of nuclease free water. The mixture was then carefully transferred into a sterile PCR strip tube (avoid bubbles formation) and centrifuged using microcentrifuge for 5 seconds to remove the excess air bubbles in the PCR mastermix. These steps were repeated for all genes of interest. Each gene was assayed in triplicate.

The expression of genes of interest was analysed using StepOnePlus Real-Time PCR system. A total of 40 amplification cycles was performed, with each cycle consisting of 5 seconds at 95°C (denaturation step), followed by 20 seconds at 60°C (annealing and extension steps). A melting curve was generated using the Applied Biosystems real-time PCR system software. The data was then normalized to GAPDH as the housekeeping gene. The relative mRNA expression was calculated using the formula in Equation 3,

Relative mRNA expression = $2^{\Delta\Delta C_q}$ (3)

Where,

$^{\Delta\Delta C}_q$ = $C_q$ housekeeping gene – $C_q$ gene of interest

$C_q$ = Threshold cycle; relative measure of the mRNA expression level

### 3.2.7 DEP Biosensor Technique

DEP biosensor was used to study the dielectrical properties (cell membrane charges) of the WRL68 and HepG2 cells. The operating procedure of DEP device used in this study was adapted from a study done by a research team of Department of Biomedical Engineering, Faculty of Engineering, University of Malaya (Yafouz, Kadri & Ibrahim, 2013). This technique was essential to differentiate the cancerous liver cells from normal liver cells and determine the effect of treatments on the liver cancer cells, HepG2. DEP analysis was performed in complement with the bioassay analyses to study the post-treatment cellular properties.

#### 3.2.7.1 DEP Device Setup

The device is made up of 5 layers, consisting of top and bottom layers, and gold dot microelectrode, a spacer and an indium tin oxide (ITO) layer sandwiched in between. Each layer was carefully assembled in the arrangement illustrated in Figure 2.3(a).

### 3.2.7.2 Preparation of DEP Medium

DEP medium was prepared by dissolving 12.7 g of D-mannitol in 250 mL deionized water. This step was sped up using magnetic stirrer. The second solution needed for preparation of DEP medium is 100 mM potassium chloride (KCl) solution in which 3.75 g of KCl was dissolved in 500 mL deionized water. KCl solution was carefully dripped into the D-mannitol solution using sterile pastuer pipette until the medium conductivity achieved 100 µS/cm.

### 3.2.7.3 Microscopic DEP Analysis

WRL68 cells were plated at $2 \times 10^6$ cells per well into a sterile 6-well plate (one well only), while the remaining 5 wells were seeded with similar volume of HepG2 cells. WRL68 and one well of HepG2 cells were left untreated while the other 4 wells of HepG2 cells each was treated with $IC_{50}$ of each treatment (KGM, D-mannose, KGM-D-mannose and 5-FU) and incubated in 5% $CO_2$ incubator for 24 hours.

After treatment, cell suspension was prepared (followed steps in Section 3.2.1.1 Subculture of Cell Lines) but the cell pellet was resuspended in DEP medium for DEP analysis. Approximately 10 µL ($2 \times 10^4$ cells) cell suspension was loaded into the spacer of DEP device. The movement of cells before and after DEP effects were observed using phase contrast inverted microscopy technique. The original cells position (pre-current cell image) was captured using Nikon ECLIPSE Ti-S microscopy camera software. The gold microelectrode and ITO (ground electrode) were then connected to the current source with 220 kHz frequency. The frequency used in this study was 220 kHz, the crossover frequency for normal liver cell line, WRL68 as reported by Yafouz et al. (2016). The movement of cells upon DEP effect was observed

under phase contrast inverted microscope at 4× magnification and post-current cell image was captured. The pre- and post-current cell images were further analysed for the DEP effects on cells (positive, negative or no DEP effects) using MATLAB software.

#### 3.2.7.4 Quantitative DEP Analysis using MATLAB

The microscopic images obtained were analysed to determine the value of light intensity shift and quantify the DEP force applied to each cells population. The image was segmented into region of interest (ROI), which is the central part of the dot area on the microelectrode. The ROI was segmented in square shape with the dimensions of 85 × 85 pixels.

The image was then converted into binary which consist only black and white counterpart using the build-in function 'im2bw' in MATLAB as illustrated in Figure 3.3. The function accepts two parameters, the image itself and a 'level' value. The 'level' value was determined using Otsu's method, in which the threshold value (ranging from 0 to 1) was chosen. The value was then used to determine the intensity level boundary in which anything less than value is converted to '0' (black) and anything more is '1' (white). Lastly, the total of black pixels for each image was calculated to determine the light intensity. The light intensity shift was calculated by subtracting the total black pixels of initial image (without signal applied to cells) from the total black pixels of final image (with signal applied to cells).

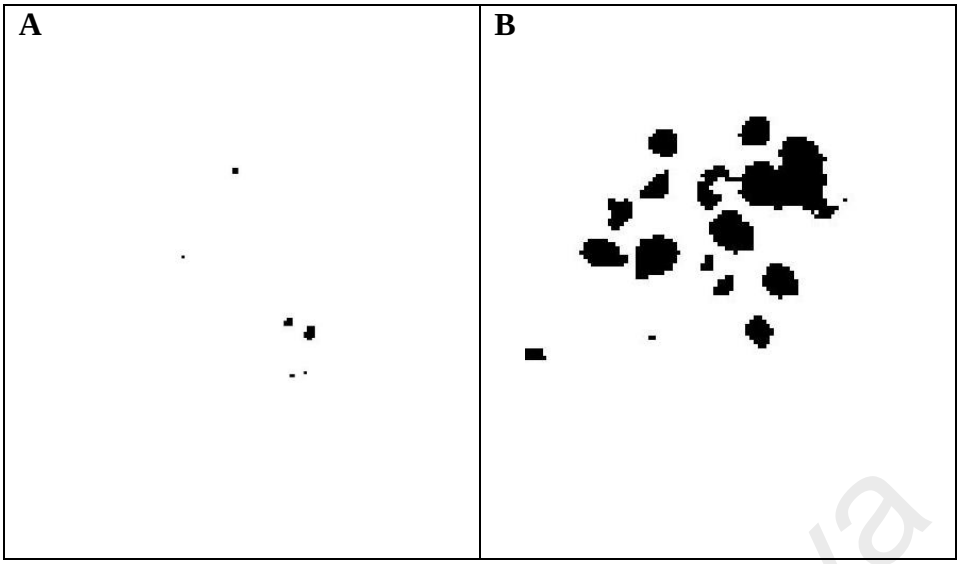


**Figure 3.3:** Illustration of segmented image converted into binary, (A) before application of signal, (B) after application of signal

### 3.3 Statistical Analysis

All the experimental groups were tested for n=3 independent experiment. Quantitative data were analysed using GraphPad Prism 5.0 to obtain means, standard deviation and standard error. Independent sample t-test was carried out to determine the statistical significance in which P value $< 0.05$ is indicated to be statistically significant.

# CHAPTER 4

# RESULTS

The research findings are tabulated in tables and figures, along with complete descriptions. Results are presented in sub-topics in which each represents specific parameter tested in this study namely morphological evaluation, cytotoxicity effect, apoptosis detection, gene expression analysis as well as dielectric changes in both HepG2 and WRL68 cells.

## 4.1 Post-treatment Morphological Changes in HepG2 and WRL68 Cells

Untreated HepG2 cells shown in Figure 4.1 displayed its epithelial structure characterised by a well-preserved plasma membrane. Konjac glucomannan (KGM) treated HepG2 cells however, exhibited apoptotic characteristics mimicking 5-Fluorouracil (5-FU) treated cells as depicted by the irregular outline of plasma membrane, reduction in size and present of membrane-bound apoptotic bodies at all incubation periods as indicated in the Figure 4.1. Both HepG2 and WRL68 cells treated with combination of KGM-D-mannose did not express obvious morphological changes as compared to control (untreated cells). D-mannose treatment supported the growth and proliferation in both cell lines. Clear reduction in size and number of WRL68 cells was seen after treatment with 5-FU in time-dependent manner (Figure 4.2). Loss of adhesion of some 5-FU treated WRL68 cells indicating the possibility of apoptosis occurrence on normal liver cells upon treatment with standard chemotherapeutic drug as pointed by the arrows in Figure 4.2.

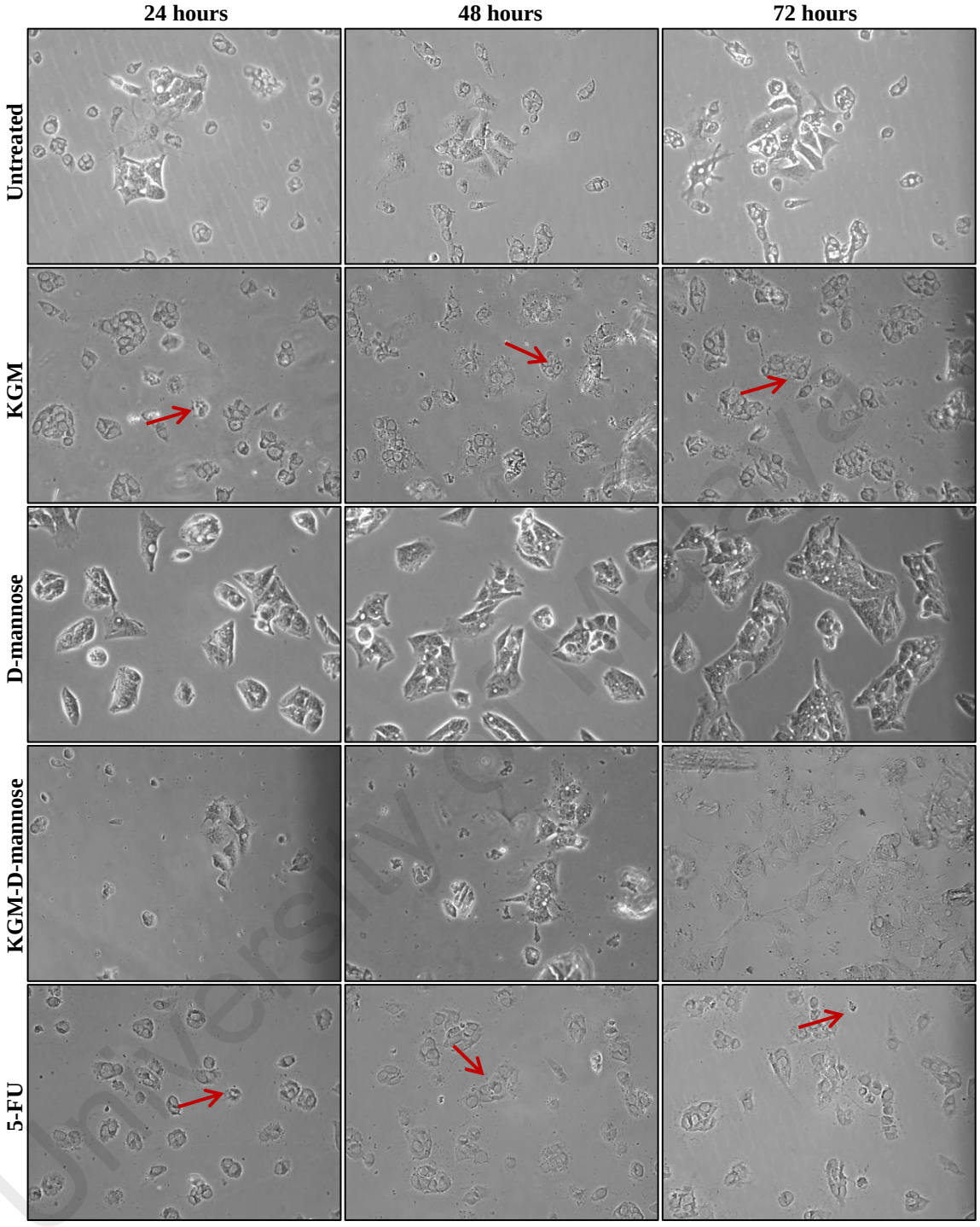


**Figure 4.1:** Representative figures of morphological changes in HepG2 cells before and after treatment with 5 mg/mL of KGM, D-mannose and KGM-D-mannose and 10 µg/mL of 5-FU (positive control) for 24, 48 and 72 hours. These morphological changes of the treated and untreated cells were captured using phase contrast inverted microscope (Nikon ECLIPSE Ti-S) at 200× magnification. The arrow indicates the apoptosis-like occurrence in HepG2 cells after treatment

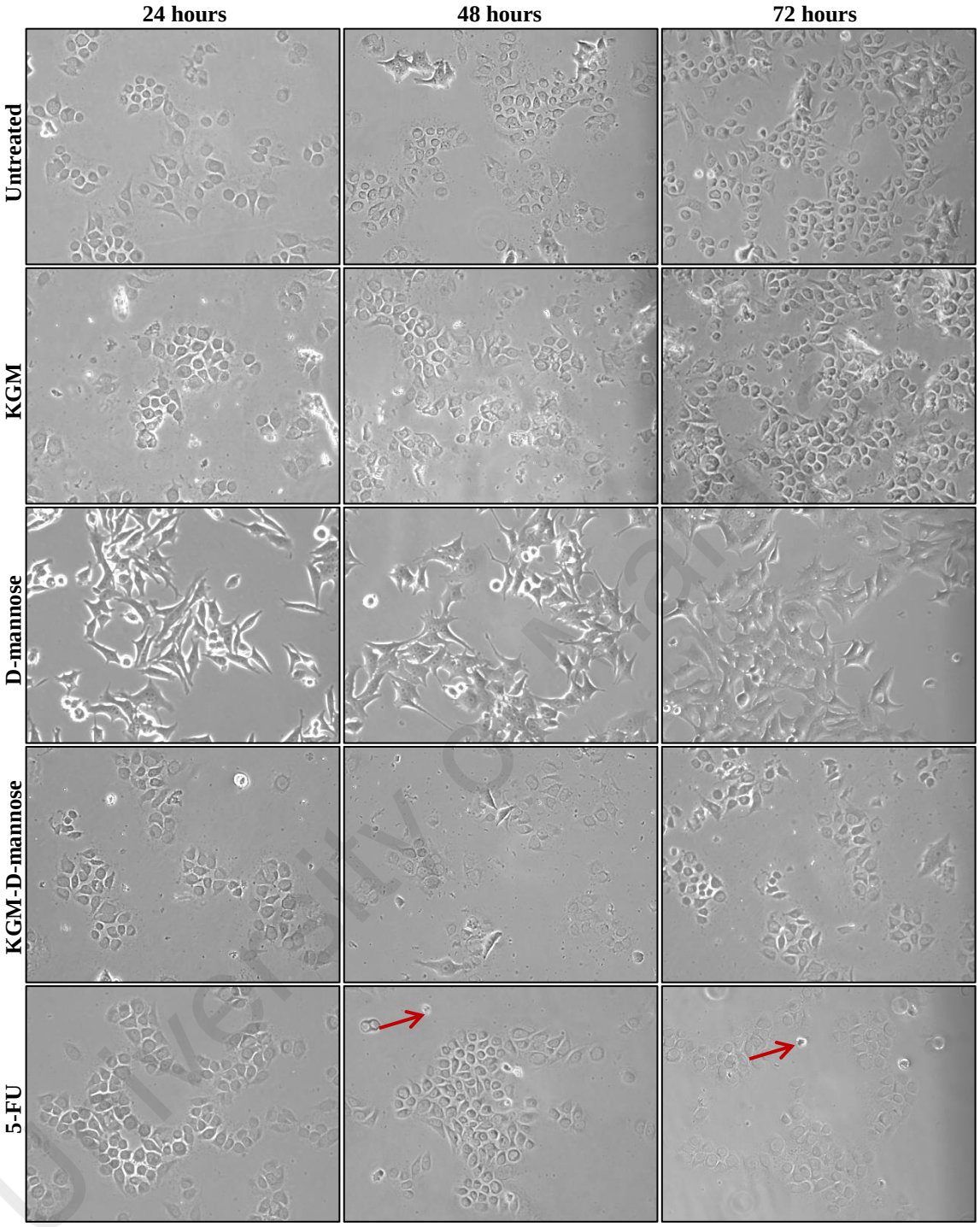


**Figure 4.2:** Representative figures of morphological changes in WRL68 cells before and after treatment with 5 mg/mL of KGM, D-mannose and KGM-D-mannose and 10 µg/mL of 5-FU (positive control) for 24, 48 and 72 hours. These morphological changes of the treated and untreated cells were captured using phase contrast inverted microscope (Nikon ECLIPSE Ti-S) at 200× magnification. The arrow indicates the apoptosis-like occurrence in WRL68 cells after treatment

## 4.2 Cytotoxic Effect of Treatments on HepG2 and WRL68 Cells Viability

KGM and KGM-D-mannose treatments significantly reduced ($p<0.05$) HepG2 cells metabolic activity at 24 hours, but not at 48 and 72 hours incubation as assessed by MTT assay in Figure 4.3. However, only KGM expressed no significant difference as compared to the standard treatment (5-FU) with P value = 0.53 ($p>0.05$). Based on Table 4.1, KGM inhibited the viability of HepG2 cells in concentration-dependent manner at all incubation periods in which the lowest cell viability was shown in 5 mg/mL KGM treatment with 38±5.598% at 24 hours, while no significant reduction in HepG2 cell viability at 48 and 72 hours as compared to control (untreated).

There is slight reduction in the viability of HepG2 cells at 24, 48 and 72 hours upon D-mannose treatment with no significant difference to negative control (untreated). KGM-D-mannose showed better inhibition than D-mannose at 24 hours with the lowest cell viability of 58±5.657% at 5 mg/mL as shown in Table 4.1. The positive control 5-FU exhibited the highest inhibition effect in time-dependent manner. It inhibited more than 50% of HepG2 cells at the concentration as low as 2 µg/mL at 48 hours and as incubation time increases, the percentage of viable cells significant reduced.

Half-maximal inhibitory concentration ($IC_{50}$) of each treatment was obtained from the graphs in Figure 4.3 at 24 hours as displayed in Table 4.2. Overall, KGM exhibited the highest cytotoxic effect in HepG2 cells with $IC_{50}$ of 3.60 mg/mL, followed by KGM-D-mannose ($IC_{50}$ ~6.95 mg/mL) and the least was D-mannose ($IC_{50}$ ~7.25 mg/mL). The $IC_{50}$ of standard drug 5-FU is 4.00 µg/mL.

**Table 4.1:** Percentage viability of HepG2 cells after KGM, D-mannose, KGM-D-mannose and 5-FU treatments at 24, 48 and 72 hours

| Treatments | Concentration (mg/mL) | Percentage of cell viability (%) | | |
|---|---|---|---|---|
| | | 24 hours | 48 hours | 72 hours |
| KGM | 1.0 | 83 ± 3.899 | 83 ± 4.469 | 81 ± 7.082 |
| | 2.0 | 62 ± 2.298 | 77 ± 5.866 | 84 ± 5.155 |
| | 3.0 | 59 ± 2.232 | 68 ± 1.790 | 79 ± 4.435 |
| | 4.0 | 40 ± 7.068 | 70 ± 3.150 | 71 ± 1.676 |
| | 5.0 | 38 ± 5.598 | 71 ± 4.567 | 70 ± 6.772 |
| D-mannose | 1.0 | 77 ± 1.369 | 82 ± 1.008 | 74 ± 2.159 |
| | 2.0 | 79 ± 2.204 | 91 ± 7.853 | 78 ± 3.016 |
| | 3.0 | 82 ± 2.465 | 99 ± 3.378 | 85 ± 1.528 |
| | 4.0 | 78 ± 1.546 | 96 ± 1.308 | 95 ± 5.963 |
| | 5.0 | 76 ± 2.207 | 92 ± 4.601 | 94 ± 9.491 |
| KGM-D-mannose | 1.0 | 85 ± 5.923 | 83 ± 3.602 | 88 ± 3.919 |
| | 2.0 | 70 ± 6.462 | 80 ± 0.980 | 84 ± 4.318 |
| | 3.0 | 63 ± 3.894 | 78 ± 3.099 | 81 ± 2.034 |
| | 4.0 | 61 ± 1.194 | 76 ± 3.326 | 86 ± 6.385 |
| | 5.0 | 58 ± 5.657 | 78 ± 3.664 | 84 ± 4.075 |

Data are expressed as mean ± standard deviation (SD), (n= 3).

**Table 4.1, continued:** Percentage viability of HepG2 cells after KGM, D-mannose, KGM-D-mannose and 5-FU treatments at 24, 48 and 72 hours

| Treatments | Concentration (µg/mL) | Percentage of cell viability (%) | | |
|---|---|---|---|---|
| | | 24 hours | 48 hours | 72 hours |
| 5-FU | 2.0 | 74 ± 8.130 | 44 ± 9.836 | 21 ± 1.279 |
| | 4.0 | 51 ± 7.646 | 29 ± 2.896 | 13 ± 2.168 |
| | 6.0 | 42 ± 8.720 | 21 ± 4.902 | 11 ± 3.661 |
| | 8.0 | 40 ± 8.712 | 15 ± 2.925 | 9 ± 1.584 |
| | 10.0 | 40 ± 13.565 | 12 ± 3.350 | 7 ± 0.220 |

Data are expressed as mean ± standard deviation (SD), (n= 3).

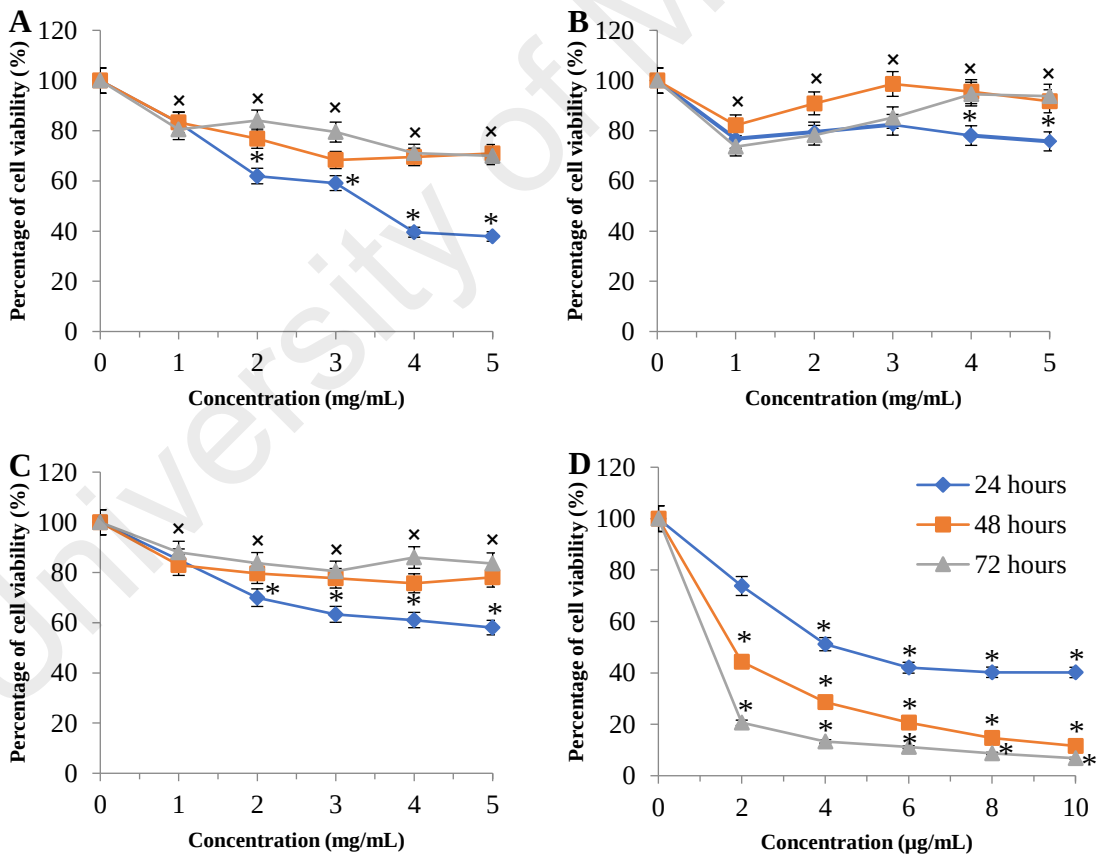


**Figure 4.3:** The percentage viability of HepG2 cells treated with various concentrations of (A) KGM, (B) D-mannose, (C) KGM-D-mannose and (D) 5-FU, respectively for 24, 48 and 72 hours. *, × indicate significant difference between (a) treatments and control (untreated), (b) treatments and positive control 5-FU, respectively, with $p<0.05$

**Table 4.2:** $IC_{50}$ values for treatments and positive control

| **Treatment/ Positive control** | **$IC_{50}$** |
|---|---|
| KGM | 3.60 mg/mL |
| D-mannose | ~7.25 mg/mL |
| KGM-D-mannose | ~6.95 mg/mL |
| 5-FU | 4.00 µg/mL |

~: Approximate $IC_{50}$ value (x) was obtained via the substitution of the respective values into the non-quadratic line equation $y = mx + c$.
Where, y = 50% of cell viability; c = constant y-intersection at 70%; m = gradient of the curves of -2.76 and -2.88 for D-mannose and KGM-D-mannose, respectively.

KGM, D-mannose and KGM-D-mannose did not inhibit the viability of normal liver cell line, WRL68 in which the percentage viability of WRL68 cells significantly increased ($p<0.05$) with the supplementation of all treatments as compared to negative control (untreated). The percentage of viable WRL68 cells increased with increased concentration of KGM treatment at 24 and 48 hours, at 72 hours the percentage viability increased at 1 mg/mL of KGM and reached plateau at 3 mg/mL as shown in Table 4.3. Similar effect was presented in KGM-D-mannose combination treatment.

Significant rise in WRL68 cells viability was observed in D-mannose treatment in which the viability achieved plateau at approximately 3 mg/mL with percentages of 154±2.089% and 155±1.874% at 24 and 48 hours, respectively as illustrated in Figure 4.4. The inhibitory effect of 5-FU on WRL68 cells metabolic activity however, significantly increased after longer incubation period (72 hours) in concentration-dependent manner with the lowest viability of 41±2.260% at 10 µg/mL as shown in Table 4.3.

**Table 4.3:** Percentage viability of WRL68 cells after KGM, D-mannose, KGM-D-mannose and 5-FU treatments at 24, 48 and 72 hours

| Treatments | Concentration (mg/mL) | Percentage of cell viability (%) | | |
|---|---|---|---|---|
| | | 24 hours | 48 hours | 72 hours |
| KGM | 1.0 | 119 ± 5.334 | 112 ± 0.497 | 90 ± 3.659 |
| | 2.0 | 132 ± 0.543 | 113 ± 0.226 | 86 ± 2.703 |
| | 3.0 | 137 ± 1.241 | 115 ± 0.944 | 91 ± 2.418 |
| | 4.0 | 147 ± 4.566 | 116 ± 1.100 | 90 ± 2.123 |
| | 5.0 | 153 ± 0.803 | 119 ± 2.206 | 90 ± 2.326 |
| D-mannose | 1.0 | 156 ± 0.908 | 113 ± 3.221 | 102 ± 3.597 |
| | 2.0 | 151 ± 2.861 | 127 ± 1.346 | 115 ± 2.828 |
| | 3.0 | 154 ± 2.089 | 155 ± 0.042 | 116 ± 1.645 |
| | 4.0 | 155 ± 2.899 | 155 ± 1.874 | 119 ± 5.393 |
| | 5.0 | 155 ± 3.141 | 155 ± 3.425 | 130 ± 3.177 |
| KGM-D-mannose | 1.0 | 128 ± 0.967 | 121 ± 0.197 | 100 ± 3.057 |
| | 2.0 | 133 ± 1.328 | 122 ± 1.196 | 105 ± 1.616 |
| | 3.0 | 140 ± 7.415 | 125 ± 2.358 | 108 ± 2.948 |
| | 4.0 | 145 ± 0.327 | 131 ± 0.712 | 112 ± 2.567 |
| | 5.0 | 156 ± 8.830 | 138 ± 2.510 | 115 ± 3.149 |

Data are expressed as mean ± standard deviation (SD), (n= 3).

**Table 4.3, continued:** Percentage viability of HepG2 cells after KGM, D-mannose, KGM-D-mannose and 5-FU treatments at 24, 48 and 72 hours

| Treatments | Concentration (µg/mL) | Percentage of cell viability (%) | | |
|---|---|---|---|---|
| | | 24 hours | 48 hours | 72 hours |
| 5-FU | 2.0 | 100 ± 0.305 | 76 ± 1.560 | 61 ± 3.865 |
| | 4.0 | 95 ± 0.860 | 74 ± 7.250 | 54 ± 1.375 |
| | 6.0 | 93 ± 0.295 | 71 ± 3.430 | 53 ± 3.750 |
| | 8.0 | 80 ± 2.000 | 70 ± 1.850 | 52 ± 3.750 |
| | 10.0 | 73 ± 3.530 | 65 ± 9.065 | 41 ± 2.260 |

Data are expressed as mean ± standard deviation (SD), (n= 3).

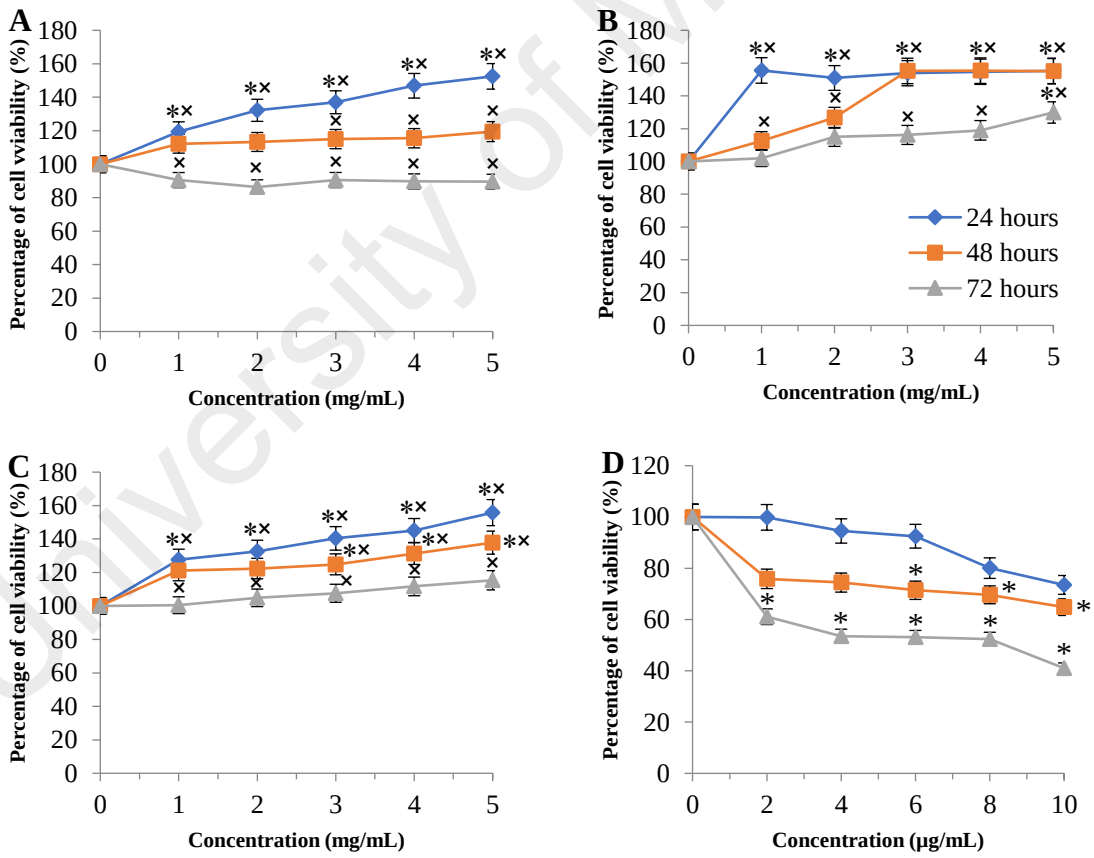


**Figure 4.4:** The percentage viability of WRL68 cells treated with various concentrations of (A) KGM, (B) D-mannose, (C) KGM-D-mannose and (D) 5-FU, respectively for 24, 48 and 72 hours. *, × indicate significant difference between (a) treatments and control (untreated), (b) treatments and positive control 5-FU, respectively, with $p<0.05$

### 4.3 Apoptosis in HepG2 and WRL68 Cells Treated with $IC_{50}$ of Treatments

Dot-plots analysis allowed detection of apoptosis in cells at different stages namely early apoptosis in lower right (LR) quadrant, late apoptosis in upper right (UR) quadrant and necrosis in upper left (UL) quadrant while viable cells were presented in lower left (LL) quadrant as shown in Figure 4.5. Higher HepG2 cell population in LR, UR and UL quadrants was observed in KGM, D-mannose and KGM-D-mannose treatments indicating higher apoptotic and necrotic events in HepG2 cells. On the contrary, low apoptosis and necrosis in WRL68 after treated with KGM, D-mannose and KGM-D-mannose evidenced by high viable cell percentage with 85.0, 85.9 and 88.3%, respectively, which showed no obvious difference as compared to untreated WRL68 cells (88.0% viable rate). Standard drug, 5-FU however, induced high cell death in both cell lines (Figure 4.5).

The highest apoptotic (early and late apoptosis) and necrotic events was shown in HepG2 cells treated with 5-FU, followed by D-mannose, KGM and the least was KGM-D-mannose-treated with the total percentage of dead cells of 56.17±1.67%, 56.00±1.21%, 54.83±4.39% and 48.40±2.77%, respectively (Figure 4.6A). Cellular apoptosis in HepG2 cells increased significantly ($p<0.05$) with all treatments compared to control. Treatment with chemotherapeutic drug, 5-FU significantly induced cell death in WRL68 cells by 41.67±1.44%, $p< 0.05$ (Figure 4.6B) while all the other three treatments did not induce significant apoptotic and necrotic effects on normal liver cell line, WRL68 (KGM, 13.70±1.74%; D-mannose, 13.83±0.46%; KGM-D-mannose, 12.47±1.42%) as compared to untreated WRL68 cells with 11.23±1.16% total cell death. Overall, supplementations of KGM, D-mannose and KGM-D-mannose showed selective inhibitions on viability of HepG2 cells, but not WRL 68 cells. However, 5-FU did affect the viability of both cancer and normal liver cell lines.

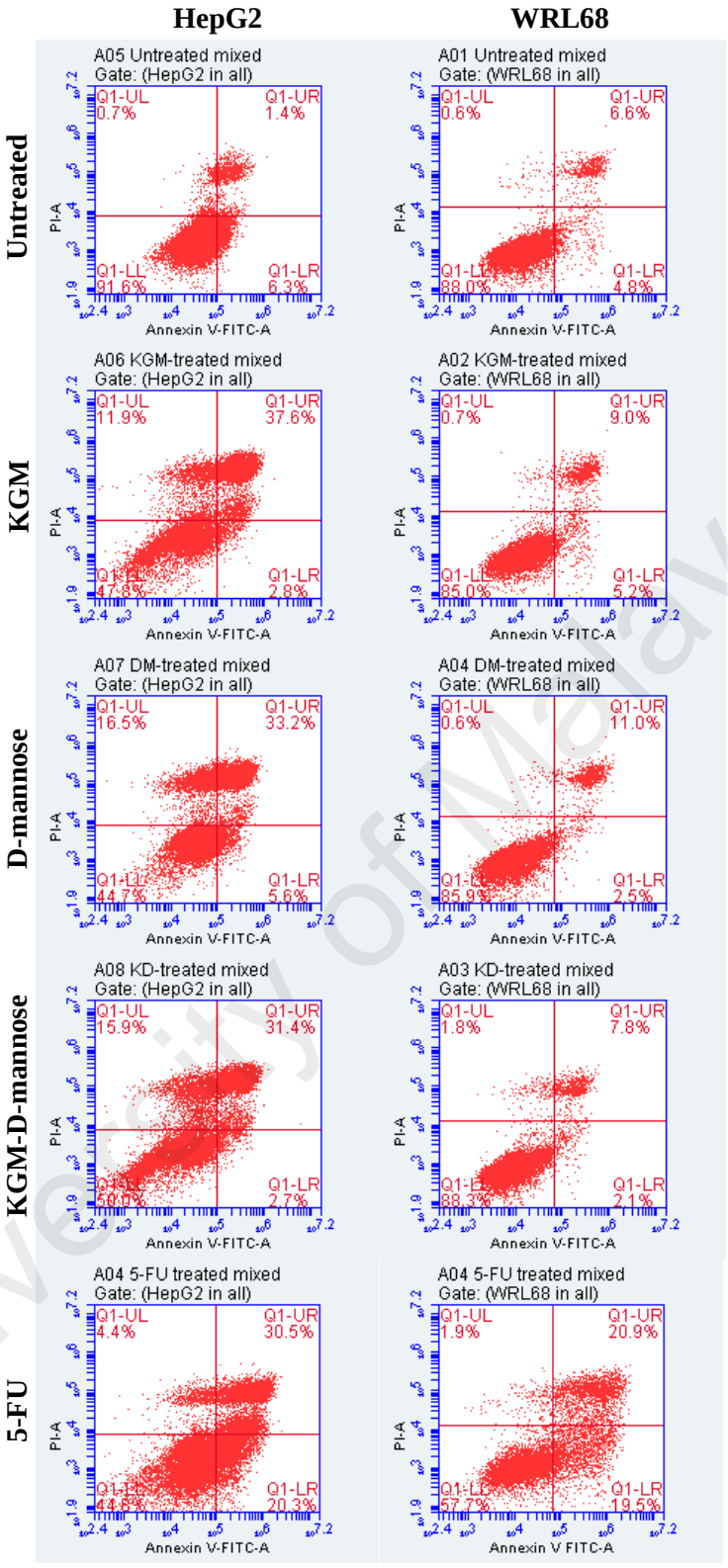


**Figure 4.5:** Representative dot-plot of Annexin V-FITC apoptosis detection assay using flow cytometry analysis. Non-apoptotic (LL - negative FITC Annexin V, negative Propidium Iodide, PI), early apoptotic (LR - positive FITC Annexin V, negative PI), late apoptotic (UR - positive FITC Annexin V, positive PI) and necrosis (UL - negative FITC Annexin V, positive PI)

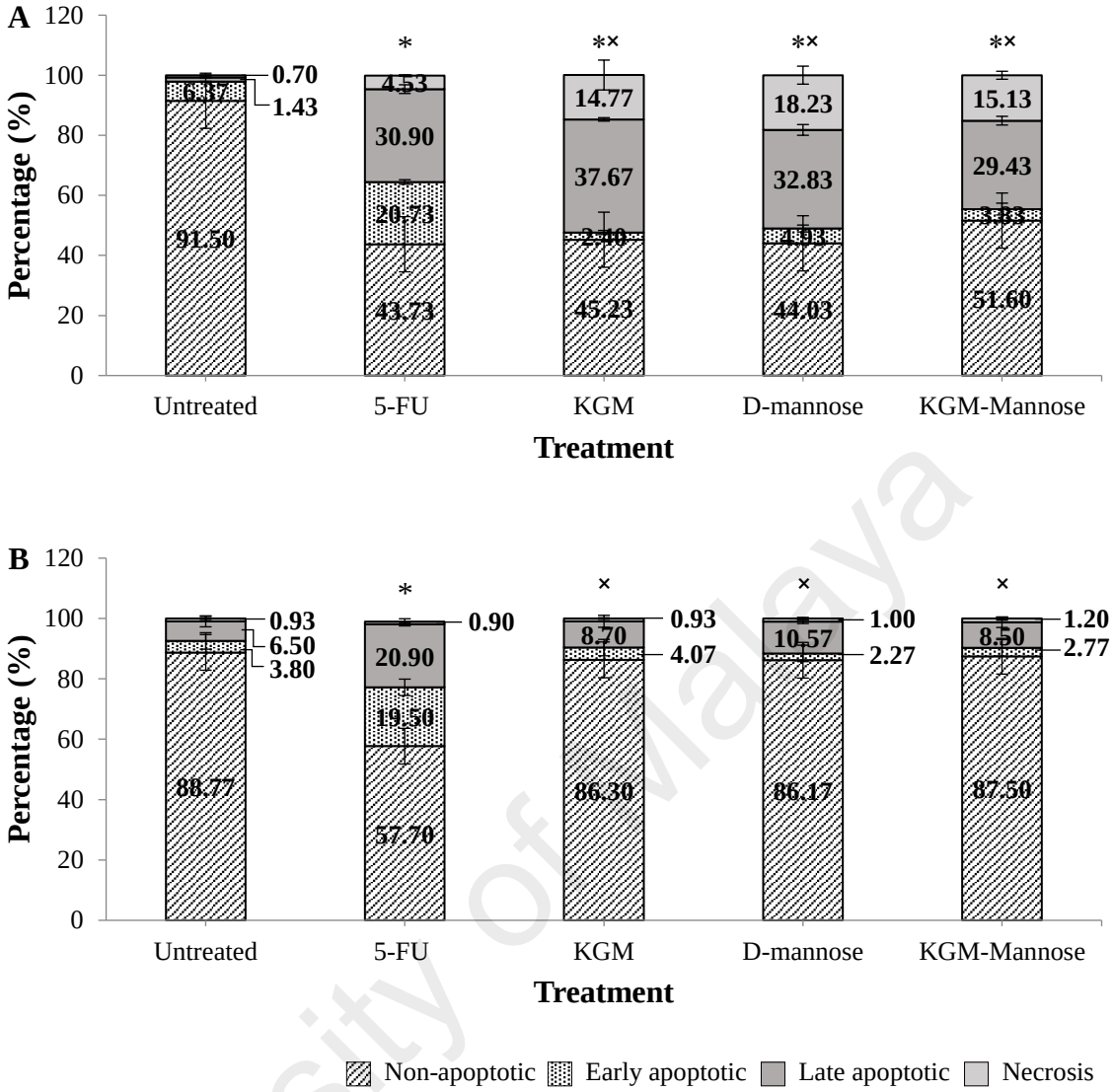


**Figure 4.6:** The post-treatments percentage of non-apoptotic, early apoptotic, late apoptotic and necrosis (A) HepG2 and (B) WRL68 cells, respectively, for 24 hours. Both cells were treated with $IC_{50}$ of each treatment: 3.60 mg/mL KGM, 7.25 mg/mL D-mannose, 6.95 mg/mL KGM-D-mannose and 4.00 µg/mL 5-FU. Results shown represent mean ± standard deviation (n=3), *, × indicate significant difference in total apoptosis between (a) treatments and control (untreated), (b) treatments and positive control 5-FU, respectively, with $p<0.05$

### 4.4 Post-treatment Effects on Apoptotic and Proliferative Genes Expression

The effect of KGM, D-mannose, KGM-D-mannose and 5-FU treatments on expression of apoptosis genes was then evaluated. Figure 4.7 depicted that KGM treatment significantly up-regulated ($p<0.05$) the expression of BAX (pro-apoptotic) and p16 (cell cycle inhibitor) genes in HepG2 cells by 2 and 4 folds, respectively. Similarly in 5-FU-treated HepG2 cells, p16 gene expression increased by 10 folds with significant 3 folds difference compared to KGM; while BAX gene expressed no significant changes but twice higher in KGM treatment. BCL2, p16 and CyclinD1 showed no significant fold change as compared to negative and positive controls. In contrast, D-mannose-treated HepG2 cells showed significant decreased in expression of BAX and p53, while gene related to cell cycle progression, Cyclin D1 increased by 2 folds compared to both untreated and positive control 5-FU-treated ($p<0.05$). The expression level of all genes did not show significant changes in HepG2 cells treated with combination of KGM-D-mannose.

Conversely, WRL68 cells exhibited significant reduction ($p<0.05$) in the expression of BCL2, BAX and p16 associated with up-regulation of Cyclin D1 after KGM and D-mannose treatments. P53 expression significantly reduced in D-mannose-treated WRL68 cells while other treatments showed no significant changes as compared to negative control (untreated). KGM-D-mannose combination however did not induce any significant changes in all genes of interest. Significant increase in the expression of p53 and p16 genes, accompanied with down-regulation of BCL2 gene were observed in 5-FU-treated WRL68 cells ($p<0.05$). The changes in expression of genes of interest in WRL68 cells treated with KGM, D-mannose and KGM-D-mannose significantly differ to the 5-FU.

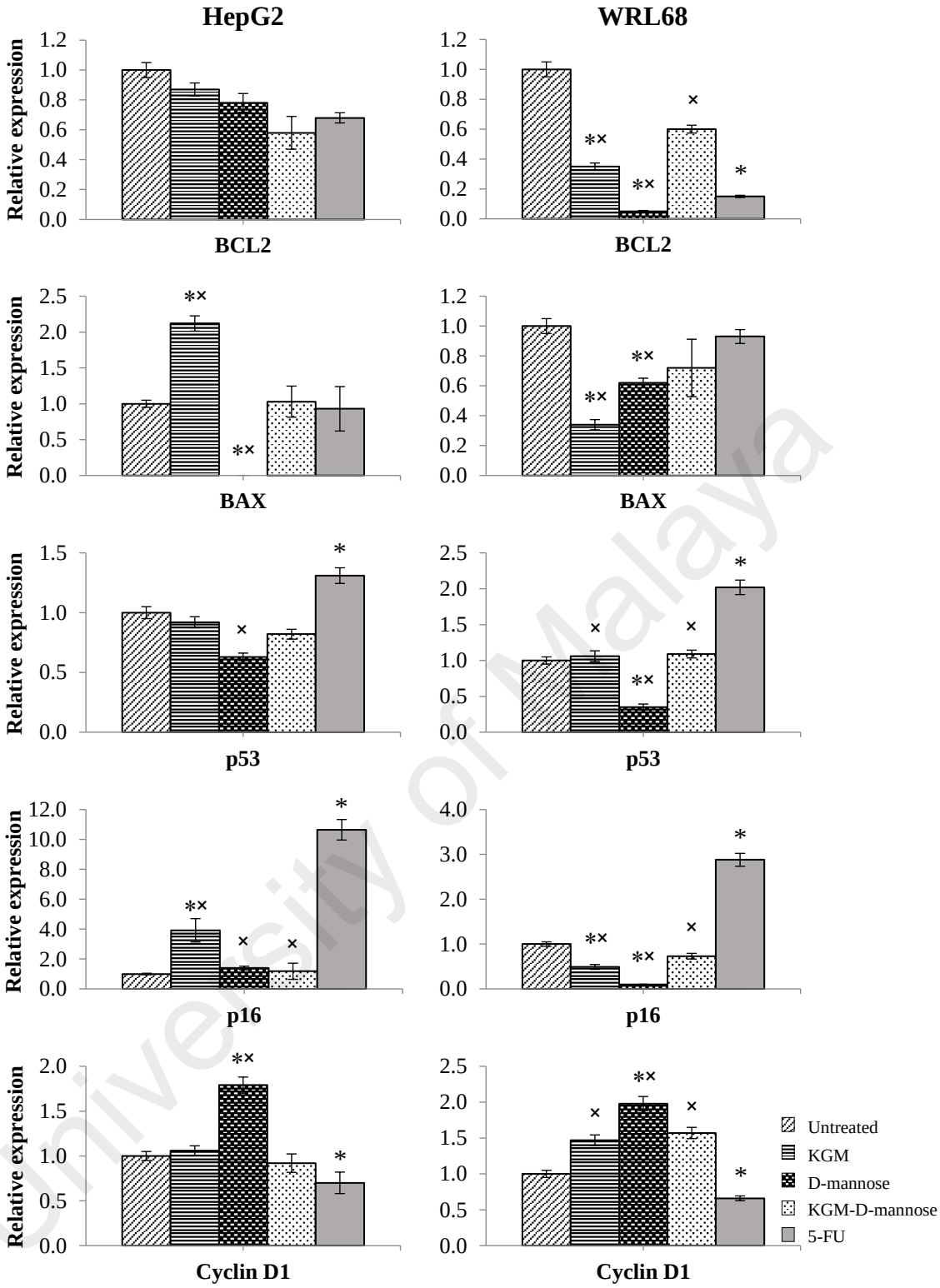


**Figure 4.7:** Relative expression of BCL2, BAX, p53, p16 and Cyclin D1 genes in HepG2 and WRL68 cells treated with $IC_{50}$ of each treatment: 3.60 mg/mL KGM, 7.25 mg/mL D-mannose, 6.95 mg/mL KGM-D-mannose and 4.00 µg/mL 5-FU. Results shown represent mean ± standard deviation (n=3), *, × indicate significant difference between (a) treatments and control (untreated), (b) treatments and positive control 5-FU, respectively, with $p < 0.05$

## 4.5 DEP Biosensor Analyses

### 4.5.1 Microscopic DEP Analysis

The DEP crossover frequency of human hepatic cell line, WRL68 is 220 kHz (Yafouz et al., 2016), which was used as the standard frequency to determine the DEP effects on hepatocellular carcinoma cell line, HepG2, before and after treatments. DEP crossover frequency refers to no resultant movement of cells in response to DEP force (Yafouz et al., 2016). Figure 4.8 depicted the differences in DEP properties between normal and cancer liver cell lines in response to the same signal (220 kHz) by assessing the movement of the cells around the dot area of the microelectrode. WRL68 cells were distributed homogenously over the dot area (centre) on microelectrode and remain unchanged after applying the signal, indicated no DEP effect (Figure 4.8B). HepG2 cells however, experienced negative DEP (n-DEP) evidenced by movement towards the dot centre as pointed by the arrows in Figure 4.8D.

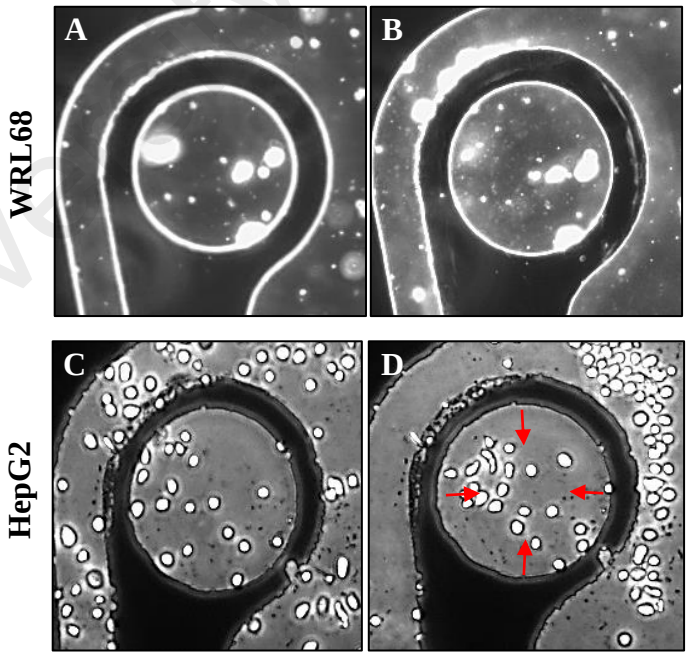


**Figure 4.8:** DEP effects on human hepatic cell line, WRL68 and hepatocellular carcinoma cell line, HepG2. Both cells were observed and captured using inverted microscope (Nikon ECLIPSE Ti-S) at 4× magnification before and after applying 220 kHz signal. WRL68 cells (A) before and (B) after applying 220 kHz signal; HepG2 cells (C) before and (D) after applying 220 kHz signal. The arrows indicate the movement of cells upon application of current

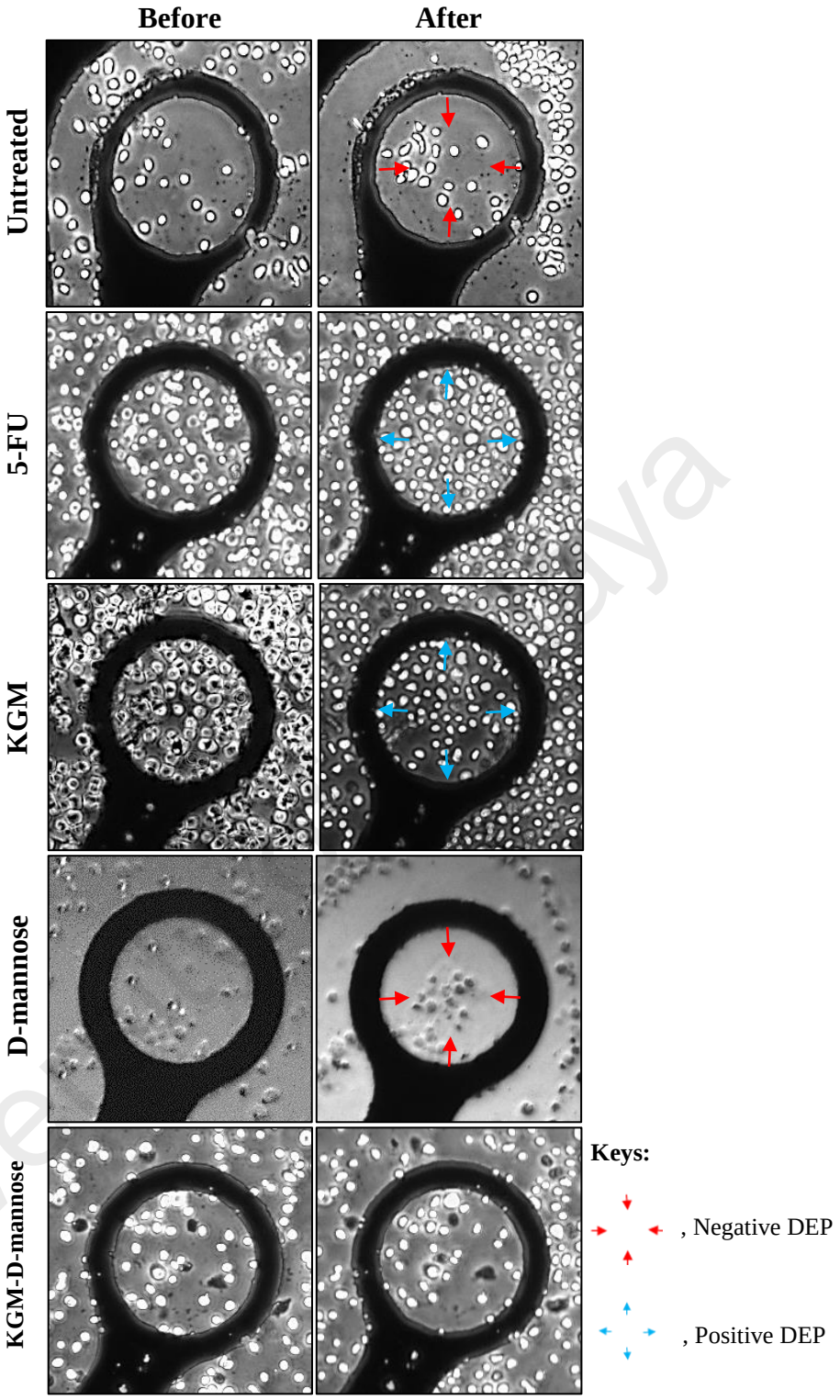


**Figure 4.9:** DEP effects on hepatocellular carcinoma cell line, HepG2 before and after applying 220 kHz signal. The cells were treated with $IC_{50}$ of treatments: 4.00 µg/mL 5-FU (positive control), 3.60 mg/mL KGM, 7.25 mg/mL D-mannose and 6.95 mg/mL KGM-D-mannose, respectively. DEP effects on cells were observed and captured using inverted microscope (Nikon ECLIPSE Ti-S) at 4× magnification. The arrows indicate the movement of cells upon application of current

DEP biosensor was further used to study the effect of treatments on HepG2 cells. The cells were treated with $IC_{50}$ of each treatment: 4.00 µg/mL 5-FU (positive control), 3.60 mg/mL KGM, 7.25 mg/mL D-mannose and 6.95 mg/mL KGM-D-mannose, respectively, for 24 hours. HepG2 cells treated with 5-FU and KGM showed positive DEP effect and moved away from the dot centre as shown in Figure 4.9. D-mannose treated HepG2 cells however experienced negative DEP and accumulated at the centre of the dot. Cells treated with the combination of KGM and D-mannose showed no DEP effect after applying 220 kHz signal.

### 4.5.2 Quantitative DEP Analysis

The microscopic images were further evaluated to finalise the DEP effect in HepG2 cells which WRL68 as the negative control. This analysis also quantifies the effects of each treatment on HepG2 cells as shown in Table 4.4. Negative final DEP value indicates positive DEP (p-DEP) in which more cells move away from the dot centre of the microelectrode due to reduction in negative charges on the cell membrane and vice versa. The standard untreated WRL68 cells showed slight positive DEP (p-DEP) effect while HepG2 cells are n-DEP with the final DEP value of -14 and 598, respectively. As for the treated HepG2 cells, 5-FU (-177) and KGM (-1597) induced p-DEP effect on the cells. Meanwhile, D-mannose- and KGM-D-mannose-treated HepG2 cells are n-DEP with corresponding final DEP value of 953 and 29, respectively.

**Table 4.4:** The DEP values and DEP effects in untreated WRL68, untreated and treated HepG2 cells before and after application of 220 kHz signal

| Sample | DEP value | | Final DEP value | DEP effect |
|---|---|---|---|---|
| | Before | After | | |
| Untreated WRL68 | 947 | 933 | -14 | Positive |
| Untreated HepG2 | 406 | 1004 | 598 | Negative |
| 5-FU-treated HepG2 | 2258 | 2141 | -177 | Positive |
| KGM-treated HepG2 | 2953 | 1356 | -1597 | Positive |
| D-mannose-treated HepG2 | 32 | 985 | 953 | Negative |
| KGM-D-mannose-treated HepG2 | 1535 | 1564 | 29 | Negative |

Before: DEP value before 220 kHz signal.
After: DEP value after 220 kHz signal.
Final DEP value: DEP value obtained by subtracting the After to Before DEP values.

# CHAPTER 5

# DISCUSSION

This chapter provides interpretation and discussion of the results. The findings from the current study are compared with the discoveries from the previous works in the related fields. Further discussion of the findings and outcomes of the research is provided with literature supports in which it will be useful in determining the limitations of study and thus suggesting ways to improve the research goals in the future works.

## 5.1 Post-treatment Morphological Changes in HepG2 and WRL68 Cells

Based on the morphological evaluation, the morphological changes mimicking the apoptotic cells were observed in KGM-treated HepG2 while normal liver cells, WRL68, the morphology remain unchanged indicated that there may be selective cytotoxic properties of KGM against liver cancer cell line. KGM post-treatment cell death in HepG2 cells could be induced through inhibition in lipid metabolism. Previous findings showed the role of KGM in controlling lipid levels in human body predominantly via lipid digestion obstruction and represses hepatic cholesterol synthesis (Doi, 1995; Srikaeo & Singchai, 2016).

Plant and prebiotic fibres stimulate phosphorylation of acetyl-CoA carboxylase (ACC) resulting in malonyl-CoA build-up, a negative regulator of carnitine palmitoyltransferase 1 (CPT1). Obstruction in CPT1-dependent mitochondrial fatty acid (FA) beta-oxidation gives rise to accumulation of several saturated FAs,

monounsaturated FAs, and polyunsaturated FAs. Most liver cancer cells including HepG2 lack the vital machinery to secrete FAs and triglyceride-rich lipoprotein, thus accumulation of these compounds leading to direct toxic effects on membrane-bound organelles and plasma membrane. Inhibition of β-oxidation simultaneously depletes the vital metabolites essential in cell survival such as adenosine triphosphate (ATP) resulting in cell death (Magtanong, Ko & Dixon, 2016).

On the other hand, monosaccharide D-mannose was used as a comparative compound as previous studies reported that KGM may be recognised by a range of mannose binding receptors or lectins and activating the vital cell death machineries (Gow et al., 2011). The findings indicated that supplementation of D-mannose suppresses apoptosis and stimulates proliferation in both HepG2 and WRL68 cells. In the presence of D-mannose, HepG2 and WRL68 cells growth and proliferation increased. Cells appeared bigger in size could be due to excess accumulation of lipid droplets in cells. In addition to aerobic glycolysis, numerous cancer cells reprogrammed the mitochondrial metabolism through increased lipogenesis to satisfy the need of macromolecules synthesis (Li & Cheng, 2017).

Green et al., (2015) reported that in high sugar environment, the FA oxidation marker is suppressed leading to excess lipogenesis. Up regulation of lipogenesis in HepG2 cells shifted the lipid metabolism to esterification rather than oxidation resulting in accumulation of intracellular triglycerides (TG). HepG2 cells inability to secrete the TG-rich lipoproteins in high sugar condition could lead to morphological enlargement due to excess intracellular TG stored in lipid droplets.

## 5.2 Cytotoxic Effect of Treatments on HepG2 and WRL68 Cells Viability

MTT assay data further supported the selective inhibitory activity of KGM on HepG2 cells proliferation, while WRL68 cells viability maintained. From the current study, KGM found to have obvious cytotoxic effect against HepG2 cells at 24 hours in which it showed no significant difference as compared to standard drug (5-FU) while the other two treatments (D-mannose and KGM-D-mannose) did. At 48 and 72 hours, KGM inhibitory effect against HepG2 cells reduced mainly due to increased viscosity of fibre polymers, thus reduced the number and kinetic energy of free moving glucomannan molecules to interact with the cell surface receptors (Gawdzik, Mederska & Mederski, 2012); therefore, 24 hours had been used as the optimum incubation period for all treatments in the subsequent parameters. Based on the current findings, selective inhibitory activity of KGM may be similar to its effects on human gastric cancer cell lines SGC-7901 and AGS as reported by Chen et al. (2017), where konjac extract induced apoptosis in both cell lines. During apoptosis, the cellular fragmentation occurs, hence reduces the number of cells and vital metabolites including NADPH-dependent oxidoreductase enzymes in cells, resulting in low or no reduction of tetrazolium dye MTT to purple insoluble formazan.

On the healthy normal cells however, Wu et al., (2011) indicated that daily KGM supplementation prevents the cellular damage of human colon cells whereby the cytotoxicity of the faecal water from individual with KGM-supplemented diet reduced, resulting in protective-effect on faecal-water-induced DNA damage in colonocytes. Further, glucomannan-rich diet reduced oxidative damage on the erythrocyte membrane by increasing the proportion of unsaturated FAs in plasma membrane whereby increased unsaturation index helps maintain the fluidity of membrane hence, makes it less susceptible to oxidative stress-stimulated cell death (Kardum et al., 2014). Together

with these findings, our study suggested the protective role of KGM on normal human liver cell line WRL68 but inhibitory effect against HepG2 cells could aid in preventing or slow down the development of liver cancer. This is, however, MTT assay is a preliminary test which needs further evaluation to assess the effect of KGM compound on the underlying cell death and proliferation mechanisms.

### 5.3 Apoptosis in HepG2 and WRL68 Cells Treated with $IC_{50}$ of Treatments

Total apoptosis was seen approximately three times higher in HepG2 cells than in WRL68 for all three treatments, while 5-FU non-selectively induced apoptosis in both cell lines. In addition, KGM treatment expressed the highest total apoptotic events in HepG2 cells as compared to D-Mannose and KGM-D-mannose treatments. The post-treatment apoptosis in HepG2 cells could be due to stimulation of lipid peroxidation of polyunsaturated FAs in cells upon high saccharide environment, resulting in alteration of the organisation of lipid and protein molecules of the plasma membrane (Shaikh & Edidin, 2008).

The end product of lipid peroxidation, malondialdehyde (MDA), is a highly reactive compound that causes toxic stress in cells. A study by Zhao et al. (2016) confirmed the synergistic effect of glucose, fructose and combined fatty acids (CFA) successfully induced the metabolic disorder by altering the oxidative status in HepG2 cells. These compounds combination stimulated more production of intra- and extracellular TG and extracellular MDA, resulting in oxidative stress-induced cell death in HepG2 cells (Zhao et al., 2016).

In addition, KGM and other plant-derived dietary fibres had been reported to disrupt the bile acid metabolism in cells (Story, Furumoto & Buhman, 1997; Lattimer & Haub, 2010). Glucomannan is a viscous food additive that is commonly used as emulsifier or thickener. The viscous nature of glucomannan compound created hydrophobic interaction in the solution-gel (sol-gel) system of KGM. The intermolecular and intramolecular forces in KGM increased with the concentration leading to increase degree of deacetylation which contributes to high hydrophobic interaction to hydrogen bonding ratio (Xin et al., 2017). In agreement with their findings, KGM created the sol-gel hydrophobic environment around the cells in the culture and possibly disrupt the bile acid metabolism, thus induced the apoptosis in HepG2 cells.

The hydrophobic property of KGM sol-gel could be highly related to the ability of soluble dietary fibres to bind to bile acids *in vitro* (Kritchevsky, 1987), as well as elevate the rate of bile acids excretion *in vivo*, reducing the level of low density lipoprotein (LDL) cholesterol in hypercholesterolemic patients (Story, Furumoto & Buhman, 1997). In normal hepatocytes, the synthesised bile acids will be conjugated with glycine or taurine making them impermeable to the cell membranes upon extracellular release (Hofmann, 1999). In contrast, bile acid conjugation pathway is defective in HepG2 cells (Everson & Polokoff, 1986). Absence of glycine-conjugated bile acids and limited amount of taurine-conjugated chenodeoxycholic acid has been reported in HepG2 cells leading to the release of large amount of defective bile acid precursors and deconjugated bile acids into the extracellular environment (Einarsson et al., 2000).

The results show the significant increase in total apoptosis in HepG2 cells while WRL68 cells remained highly viable after treatment with KGM. It may be associated

with the accumulation of bile acids in the extracellular KGM sol-gel hydrophobic environment. The bile acids produced by normal hepatocytes WRL68 are hydrophobic and impermeable to the cell membrane; they bind to the KGM sol-gel making the cells unsusceptible to bile acid cytotoxicity. On the contrary, the hydrophilic bile acids precursors and deconjugated bile acids produced by HepG2 cells are capable to penetrate the cell membrane and disrupt the membrane architecture (Wu et al., 2003). Bile acid precursors are highly cytotoxic when present in abnormally high amount in which the accumulation of these compounds is greatly due to intracellular disturbances of bile acid metabolism namely defective biosynthesis and conjugation (Hofmann, 1999).

### 5.4 Post-treatment Effects on Apoptotic and Proliferative Genes Expression

To further investigate the effects of KGM, gene expression analysis was performed using real-time PCR technique to study the effect of KGM on the expression of anti-apoptotic gene (BCL2), pro-apoptotic gene (BAX), tumour suppressor gene (p53), cell cycle inhibitory gene (p16) and proliferative gene (Cyclin D1). The significant up-regulation of BAX and p16 genes associated with slight down-regulation of BCL2 gene in KGM-treated HepG2 cells similar to standard 5-FU suggested that KGM induced the apoptosis and at the same time inhibited the proliferation of liver cancer cell line. In contrast, reverse expressions of these genes were presented in KGM-treated WRL68 cells while 5-FU expressed no selective effect on both cell lines.

Apoptosis resistance in cancer cells including HCC is highly associated with overexpression of anti-apoptotic protein, Bcl-2. Bcl-2 protein binds to pro-apoptotic member, BAX, and disrupts the cytochrome release mechanism in cells. Based on the

results, KGM inhibitory effect on HepG2 cells may be expressed through activation of BAX and p16 genes but suppresses Bcl-2 protein activity upon binding to the surface receptors. High ratio of BAX to BCL2 in KGM-treated HepG2 cells is believed to disrupt the mitochondrial membrane potential, resulting in cytochrome c and caspase 9 release and eventually cell death (Naseri et al., 2015).

Furthermore, up-regulation of p16 in HepG2 cells treated with KGM could be due to the action of this compound via cell surface glycosylation pathway. Glycosylation is a complex process involving enzymes activities, organelles and extracellular factors generating carbohydrate post-translational modification of hydroxyl group of protein (Cummings & Pierce, 2014). Alteration of glycosylation in tumourigenesis facilitates rapid cell proliferation and survival, cell to cell adhesion and eventually metastasis (Stowell, Ju & Cummings, 2015). KGM is an oligosaccharide made up of D-mannose and D-glucose in a ratio of 1.6:1 (Katsuraya et al., 2003). N-linked glycosylation of oligosaccharide to the cell surface receptor induces senescence, while monosaccharide, for instance D-mannose, only provided transient cell cycle arrest (Sampathkumar et al., 2006).

In addition, aberrant expression of N-acetylglucosamine on the cancer cell surface due to hyper N-acetylation serves as the anchoring residues for glycosylation of the N-linked oligosaccharides (e.g., glucomannan and hexosamine monosaccharides). The conjugation of N-linked oligosaccharides to the cell surface receptors activates the expression of cyclin-dependent kinase (CDK) inhibitors namely p21 and p16, inhibiting the formation of Cyclin D1-CDK4/6 complex, maintaining Rb proteins in hypophosphorylated state, which then bind to E2F1, resulting in cell cycle arrest at G1 and G2 phases (Sampathkumar et al., 2006; Romagosa et al., 2011).

Gene expression analysis indicated that D-mannose treatment stimulated growth and proliferation of HepG2 and WRL68 cells by down-regulating BAX, p53 and p16 genes, and up-regulated Cyclin D1 gene. Down regulation of these genes detained the apoptotic pathways in cells. The combination of KGM-D-mannose did not show significant changes in gene expressions in HepG2 cells but induce proliferation in WRL68 cells similar to D-mannose treatment, suggesting that these two compounds may be involve in two different pathways despite they are both from saccharide family.

## 5.5 Post-treatment Dielectric Changes in HepG2 and WRL68 Cells

DEP is a phenomenon in which a neutral polarisable particle is made to move towards or away from the high field strength region upon exposure to a nonuniform electric field based on the net force that it is experiencing (Pohl, 1951; Weng et al., 2016). There are two types of DEP forces in which the particle is moving away or towards the high field strength region known as negative DEP (n-DEP) and positive DEP (p-DEP), respectively. When these two forces alternate at a specific frequency and cause the particle to remain stagnant, it is known as the crossover frequency (Ozkan et al., 2003). The crossover frequency of WRL68 normal liver cell at 220 kHz was derived and utilised in this study based on the previous work by Yafouz et al. (2016).

Microscopic and MATLAB analyses of untreated WRL68 cells at the crossover frequency showed slight p-DEP effect while untreated HepG2 cells is highly negative with a broad dielectric difference between two cell lines as shown in Table 4.4. The cell surface charges of mammal cells are negative at physiological pH in which it increases during tumourigenesis and decreases during apoptosis or necrosis. Cells that express more negative charges on the surface, for instance tumour cells (HepG2), experience n-

DEP in which they move away from the highly negative field of the DEP microelectrode. Apoptotic or necrotic cells on the other hand, experience p-DEP as their surface negative charges reduces, make them more prone to be attracted towards the high negative field (Dobrzynska, Skrzydlewska & Figaszewski, 2013). This could explain the slight p-DEP in untreated WRL68 cells due to the presence of dead cells from biological apoptosis or cell death upon cell suspension preparation.

The significant increase of p-DEP force in KGM- and 5-FU-treated HepG2 cells suggested apoptosis or necrosis in cells. D-mannose and KGM-D-mannose treatments were rather the opposite in which the cells remain in n-DEP state indicates no or little inhibitory effects of these treatments on HepG2 cells. Apoptosis and necrosis play a major role on cellular conductivity. Cell membranes are composed of lipids and can be modelled electrically by a capacitor between intra- and extracellular electrolytes. The capacitive coupling of the cell membranes allows current to pass through the membrane, which results in an increase in tissue conductivity. When cells die by apoptosis, the cell membrane damages and loses its insulating property, decreases the impedance between intra- and extracellular space, thus, tissue conductivity reduces (Haemmerich et al., 2003). The partial loss of membrane asymmetry during apoptosis generates a negative surface charge in apoptotic cells (Erwig & Henson, 2008), this is however, the membrane conductivity decreases due to diminished intramembranal ion traffic (Bonincontro et al., 1997). Overall, the dielectric changes in line with reduction in cells viability, up-regulation of apoptosis genes and down-regulation of proliferative genes in KGM-treated HepG2 cells suggested the cytotoxic nature of KGM in tumour suppression and it potentially acts via Bcl-2/BAX protein apoptosis or glycosylation pathways.

The current findings also evidenced that DEP is a simple yet rapid technique which provided immediate response without the need of biological tagging or chemical reaction on the cells. It is compatible to the molecular techniques in determining the effect of KGM, D-mannose, KGM-D-mannose and 5-FU treatments on HepG2 cell line. By referring to Table 4.4, the presence of KGM in KGM-D-mannose combination generated approximately 97% lower n-DEP effect on HepG2 cells than D-mannose alone, suggesting the ability of DEP to detect even a slight change in dielectric qualities of the cells and highly compatible as a pre-diagnostic tool for POC system

## 5.6 Strength and Limitations of the Study

The current findings signified the selective inhibition effect of KGM on HepG2 liver cancer cells, addressing the aim and objectives of the study of natural product as a safer alternative to the available liver cancer treatments, and have proven the feasibility of DEP technique in anti-cancer screening. Yet the mode of action of KGM is not explored in a comprehensive manner due to the nature of the work. The binding of KGM to the cell surface receptors or its uptake holds a promise for the further exploration.

In addition, the DEP device used in this study is limited to the time-consuming and misaligned assembly of the device which might affect the cell loading volume and vital cellular activities on-device. Therefore, future improvement is crucial to increase the device efficacy and generate high-throughput outcomes.

# CHAPTER 6

# CONCLUSION

Overall, the current findings showed that KGM selectively inhibited the proliferation and ceased the growth of HepG2 cells at $IC_{50}$ of 3.60 mg/mL but standard drug 5-FU suppressed the viability of both HepG2 and WRL68 cells at $IC_{50}$ of as low as 4.00 µg/mL. Along with clear morphological alterations, stimulation of vital apoptotic genes expression and down-regulation of the proliferative genes disclosed the effects of KGM and 5-FU treatments on the underlying cell death mechanism in HepG2 cells, potentially via mitochondria-mediated Bcl-2/BAX proteins apoptosis pathway. 5-FU however, may be involved in several pathways including p53 pathway evident by the significant up-regulation of p53 gene in both cell lines.

Non-selective inhibition of 5-FU treatment indicates the adverse effect of standard chemotherapeutic drug on non-malignant liver cell line despite the high treatment outcomes on liver cancer cells. KGM on the other hand, tumour suppressed liver cancer cell line, HepG2 and exhibited protective role on normal liver cell line, WRL68. In addition, in line with the molecular findings, the first application of DEP in assessing the post-treatment cytotoxic effect of natural compound on hepatic cancer cells showed that KGM induced apoptotic-like dielectric changes in HepG2 cells in which cells apoptosised and experienced p-DEP effect. In a nutshell, along with other clinically proven medicinal properties, this study paves a path for a further exploration of KGM as a safer preventive and selective treatment in HCC.

Consequently, anti-cancer entity of KGM via the molecular parameters in line with the alteration of dielectric quality in HepG2 cells provide insights into KGM stimulation on the underlying cell death mechanism which the relation of KGM to mannose specific receptors reported by previous studies is crucial to further validate its mechanism of action. The knowledge of the inhibitory action of KGM on HepG2 cells is indeed highly valuable for future assessment of its effectiveness against cancer stem cells and metastatic cancer cells, as well as chemo-drug resistance studies. Furthermore, tumour suppression effect of KGM on lipid and bile acid metabolisms of HepG2 cells merits future exploration. Lastly, time-effective nature of DEP warrants a complementary role in conventional laboratory tests, treatment dosage management and post-treatment monitoring in chronic diseases namely cancer, hypercholesterolemia and obesity.

## REFERENCES


Achkar, J.P., Araya, V., Baron, R.L., Marsh, J.W., Dvorchik, I., & Rakela, J. (1998). Undetected hepatocellular carcinoma: clinical features and outcomes after liver transplantation. *Liver Transplantation and Surgery*, *4*(6), 477-482.

Adams, J.M., & Cory, S. (2007). The Bcl-2 apoptotic switch in cancer development and therapy. *Oncogene*, *26*, 1324-1337.

American Cancer Society. (2016). Chemotherapy side effects. Retrieved from https://www.cancer.org/treatment/treatments-and-side-effects/treatment-types/chemotherapy/chemotherapy-side-effects.html

American Type Culture Collection. (2016). HepG2 [HEPG2] (ATCC® HB-8065™). Retrieved from https://www.atcc.org/products/all/HB-8065.aspx

American Type Culture Collection. (2016). WRL68 (ATCC® CL-48™). Retrieved from https://www.atcc.org/products/all/CL-48.aspx

Amin, A.R.M.R., Karpowicz, P.A., Carey, T.E., Arbiser, J., Nahta, R., Chen, Z.G., … Shin, D.M. (2015). Evasion of anti-growth signalling: a key step in tumourigenesis and potential target for treatment and prophylaxis by natural compounds. *Seminars in Cancer Biology*, *35*, 55-77.

Antfolk, M., Kim, S.H., Koizumi, S., Fujii, T., & Laurell, T. (2017). Label-free single-cell separation and imaging of cancer cells using an integrated microfluidic system. *Scientific Report*, *7*. Retrieved from https://www.nature.com/articles/srep46507

Bahmani, M., Shirzad, H., Rafieian, S., & Rafieian-Kopaei, M. (2015). Silybum marianum: beyond hepatoprotection. *Journal of Evidence-Based Complementary and Alternative Medicine*, *20*(4), 292-301.

Balogh, J., Victor, D., Asham, E.H., Burroughs, S.G., Boktour, M., Saharia, A., … Monsour, H.P.J. (2016). Hepatocellular carcinoma: a review. *Journal of Hepatocellular Carcinoma*, *3*, 41-53.

Baucke, V.L., Miele, E., & Staiano, A. (2004). Fibre (Glucomannan) is beneficial in the treatment of childhood constipation. *Pediatrics*, *113*(3), 259-264.

Berx, G., & van Roy, F. (2009). Involvement of members of the cadherin superfamily in cancer. *Cold Spring Harbor Perspectives in Biology*, *1*(6). http://cshperspectives.cshlp.org/content/1/6/a003129

Bolondi, L., Sofia, S., Siringo, S., Gaiani, S., Zironi, G., Piscaglia, F., …Sherman, M. (2001). Surveillance programme of cirrhotic patients for early diagnosis and treatment of hepatocellular carcinoma: a cost effectiveness analysis. *Gut*, *48*(2), 251-259.

Bonincontro, A., Iacoangeli, A., Melucci-Vigo, G., & Risuleo, G. (1997). Apoptosis dependent decrease of the intramembrane ion traffic in cultured mouse fibroblasts shown by conductivity dispersion. *Bioscience Reports*, *17*(6), 547-556.

Brahee, D.D., Ogedegbe, C., Hassler, C., Nyirenda, T., Hazelwood, V., Morchel, H., …Feldman, J. (2013). Body mass index and abdominal ultrasound image quality: a pilot survey of sonographers. *Journal of Diagnostic Medical Sonography*, *29*(2), 66-72.

Broche, L.M., Bhadal, N., Lewis, M.P., Porter, S., Hughes, M.P., Labeed, F.H. (2007). Early detection of oral cancer – is dielectrophoresis the answer? *Oral Oncology*, *43*(2), 199-203.

Busch, S.J., Barnhart, R.L., Martin, G.A., Flanagan, M.A., & Jackson, R.L. (1990). Differential regulation of hepatic triglyceride lipase and 3-hydroxy-3-methylglutaryl-CoA reductase gene expression in a human hepatoma cell line, HepG2. *The Journal of Biological Chemistry*, *265*, 22474-22479.

Canani, R.B., Di Costanzo, M., Leone, L., Pedata, M., Meli, R., & Calignano, A. (2011). Potential beneficial effects of butyrate in intestinal and extraintestinal diseases. *World Journal of Gastroenterology*, *17*(12), 1519-1528.

Cavallaro, U., & Christofori, G. (2004). Cell adhesion and signalling by cadherins and Ig-CAMs in cancer. *Nature Reviews Cancer*, *4*(2), 118-132.

Cavallaro, U., & Christofori, G. (2004). Multitasking in tumour progression: signalling functions of cell adhesion molecules. *Annals of New York Academy of Sciences*, *1014*, 58-66.

Chearskul, S., Kriengsinyos, W., & Kooptiwut, S. (2009). Immediate and long-term effects of glucomannan on total ghrelin and leptin in type 2 diabetes mellitus. *Diabetes Research and Clinical Practice*, *83*(2), 40-42.

Chen, H.L., Cheng, H.C., Liu, Y.J., Liu, S.Y., & Wu, W.T. (2006). Konjac acts as a natural laxative by increasing stool bulk and improving colonic ecology in healthy adults. *Nutrition*, *22*(11), 1112-1119.

Chen, H.L., Cheng, H.C., Wu, W.T., Liu, Y.J., & Liu, S.Y. (2008). Supplementation of konjac glucomannan into a low-fibre Chinese diet promoted bowel movement and improved colonic ecology in constipated adults: a placebo-controlled, diet-controlled trial. *Journal of the American College of Nutrition*, *27*(1), 102-108.

Chen, H.L., Sheu, W.H., Tai, T.S., Liaw, Y., & Chen, Y. (2003). Konjac supplement alleviated hypercholesterolemia and hyperglycemia in type 2 diabetic subjects - a randomized double-blind trial. *Journal of the American College of Nutrition*, *22*(1), 36-42.

Chen, X., Yuan, L.Q., Li, L.J., Lv, Y., Chen, P.F., & Pan, L. (2017). Suppression of gastric cancer by extract from the tuber of amorphophallus konjac via induction of apoptosis and autophagy. *Oncology Reports*, *38*(2), 1051-1058.

Chiao, H., Yang, C.H.E., & Frenette, C.T. (2013). Review on liver transplant for hepatocellular carcinoma. *Translational Cancer Research*, *2*(6), 472-481.

Chua, M., Baldwin, T.C., Hocking, T.J., & Chan, K. (2010). Traditional uses and potential health benefits of *Amorphophallus konjac* K. Koch ex N.E.Br. *Journal of Ethnopharmacology*, *128*, 268-278.

Colli, A., Fraquelli, M., Casazza, G., Massironi, S., Colucci, A., Conte, D., & Duca, P. (2006). Accuracy of ultrasonography, spiral CT, magnetic resonance, and alpha-fetoprotein in diagnosing hepatocellular carcinoma: a systematic review. *The American Journal of Gastroenterology*, *101*(3), 513-523.

Commane, D.M., Shortt, C.T., Silvi, S., Cresci, A., Hughes, R.M., & Rowland, I.R. (2005). Effects of fermentation products of pro- and prebiotics on trans-epithelial electrical resistance in an in vitro model of the colon. *Nutrition and Cancer*, *51*(1), 102–109.

Costantini, S., Di Bernardo, G., Cammarota, M., Castello, G., & Colonna, G. (2013). Gene expression signature of human HepG2 cell line. *Gene*, *518*(2), 335-345.

Counter, C.M., Avilion, A.A., LeFeuvre, C.E., Stewart, N.G., Greider, C.W., Harley, C.B., & Bacchetti, S. (1992). Telomere shortening associated with chromosome instability is arrested in immortal cells which express telomerase activity. *The EMBO Journal*, *11*(5), 1921-1929.

Cummings, R.D., & Pierce J.M. (2014). The challenge and promise of glycomics. *Chemistry & Biology*, *21*(1), 1-15.

Danila, M., & Sporea, I. (2014). Ultrasound screening for hepatocellular carcinoma in patients with advanced liver fibrosis, an overview. *Medical Ultrasonography*, *16*(2), 139-144.

Darvesh, A.S., Aggarwal, B.B., & Bishayee, A. (2012). Curcumin and liver cancer: a review. *Current Pharmaceutical Biotechnology, 13*(1), 218-228.

Demircan, Y., Ozgur, E., & Kulah, H. (2013). Dielectrophoresis: applications and future outlook in point of care. *Electrophoresis*, *34*(7), 1008-1027.

Di Bisceglie, A.M., Sterling, R.K., Chung, R.T., Everhart, J.E., Dienstag, J.L., Bonkovsky, H.L., …Gretch, D.R. (2005). Serum α-fetoprotein levels in patients with advanced hepatitis C: results from the HALT-C Trial. *Journal of Hepatology*, *43*(3), 434-441.

Diederichs, S., & Gutschner, T. (2012). The hallmarks of cancer along non-coding RNA point of view. *RNA Biology*, *9*(6), 703-719.

Dobrzynska, I., Skrzydlewska, E., & Figaszewski, Z.A. (2013). Changes in electric properties of human breast cancer cells. *The Journal of Membrane Biology*, *246*(2), 161-166.

Doi, K. (1995). Effect of konjac fibre (glucomannan) on glucose and lipids. *European Journal of Clinical Nutrition*, *49*(3), 190-197.

Donaldson, M.S. (2004). Nutrition and cancer: a review of the evidence for an anti-cancer diet. *Nutritional Journal*, *3*(19). https://nutritionj.biomedcentral.com/articles/10.1186/1475-2891-3-19

Einarsson, C., Ellis, E., Abrahamsson, A., Ericzon, B.G., Bjorkhem, I., & Axelson, M. (2000). Bile acid formation in primary human hepatocytes. *World Journal of Gastroenterology*, *6*(4), 522-525.

Erwig, L.P., & Henson, P.M. (2008). Clearance of apoptotic cells by phagocytes. *Cell Death and Differentiation, 15*, 243-250.

Everson, G.T., & Polokoff, M.A. (1986). HepG2, a human hepatoblastoma cell line exhibiting defects in bile acid synthesis and conjugation. *The Journal of Biological Chemistry*, *261*(5), 2197-2201.

Fang, W., & Wu, P. (2004). Variations in konjac glucomannan (KGM) from *Amorphophallus konjac* and its refined powder in China. *Food Hydrocolloids*, *18*(1), 167-170.

Forner, A., Gilabert, M., Bruix, J., & Raoul, J.L. (2014). Treatment of intermediate-stage hepatocellular carcinoma. *Nature Reviews Clinical Oncology*, *11*(9), 525-535.

Fred, H.L. (2004). Drawbacks and limitations of computed tomography. *Texas Heart Institute Journal*, *31*(4), 345-348.

Gallaher, C.M., Munion, J., Hesslink, R.J., Wise, J., & Gallaher, D.D. (2000). Cholesterol reduction by glucomannan and chitosan is mediated by changes in cholesterol absorption and bile acid and fat excretion in rats. *The Journal of Nutrition*, *130*(11), 2753-2759.

Gascoyne, P.R.C., Wang, X.B., Huang, Y., & Becker, F.F. (1997). Dielectrophoretic separation of cancer cells from blood. *IEEE Transactions on Industry Applications*, *33*(3), 670-678.

Gawdzik, A., Mederska, A., & Mederski, T. (2012). Effect of viscosity changes of reaction mixture on the kinetics of formation of linear living polymer. *Ecological Chemistry and Engineering A*, *19*(11), 1393-1403.

Gow, N.A.R., van de Veerdonk, F.L., Brown, A.J.P., & Netea, M.G. (2011). *Candida albicans* morphogenesis and host defence: discriminating invasion from colonisation. *Nature Reviews Microbiology*, *10*(2), 112-122.

Graham, K.A., Mulhall, H.J., Labeed, F.H., Lewis, M.P., Hoettges, K.F., Kalavrezos, N., …Hughes, M.P. (2015). A dielectrophoretic method of discrimination between normal oral epithelium, and oral and oropharyngeal cancer in clinical setting. *Analyst*, *140*, 5198-5204.

Green, C.J., Johnson, D., Amin, H.D., Sivathondan, P., Silva, M.A., Wang, L.M., …Hodson, L. (2015). Characterisation of lipid metabolism in a novel immortalized human hepatocyte cell line. *American Journal of Physiology, Endocrinology and Metabolism*, *309*(6), 511-522.

Gupta, M.K., & Qin, R.Y. (2003). Mechanism and its regulation of tumour-induced angiogenesis. *World Journal of Gastroenterology*, *9*(6), 1144-1155.

Gutierrez-Ruiz, M.C., Bucio, L., Souza, V., Gomez, J.J., Campos, C., & Carabez, A. (1994). Expression of some hepatocyte-like functional properties of WRL-68 cells in culture. *In Vitro Cellular & Developmental Biology – Animal*, *30A*(6), 366-371.

Haemmerich, D., Staelin, S.T., Tsai, J.Z., Tungjitkusolmun, S., Mahvi, D.M., & Webster, J.G. (2003). *In vivo* electrical conductivity of hepatic tumours. *Physiological Measurement*, *24*(2), 251-260.

Hanahan, D., & Folkman, J. (1996). Patterns and emerging mechanisms of the angiogenic switch during tumourigenesis. *Cell*, *86*(3), 353-364.

Hanahan, D., & Weinberg, R.A. (2011). Hallmarks of cancer: the next generation. *Cell*, *144*(5), 646-674.

Ho, C.T., Lin, R.Z., Chang, W.Y., Chang, H.Y., & Liu, C.H. (2006). Rapid heterogeneous liver-cell on-chip patterning via the enhanced field-induced dielectrophoresis trap. *Lab on a Chip*, *6*(6), 724-734.

Ho, C.T., Lin, R.Z., Chen, R.J., Chin, C.K., Gong, S.E., Cheng, H.Y., …Liu, C.H. (2013). Liver-cell patterning lab chip: mimicking the morphology of liver lobule tissue. *Lab on a Chip*, *13*(18), 3578-3587.

Hoeben, A., Lenduyt, B. Highley, M.S., Wildiers, H., Van Oosterom, A.T., & De Bruijn. E.A. (2004). Vascular endothelial growth factor and angiogenesis. *Pharmacological Reviews*, *56*(4), 549-580.

Hofmann, A.F. (1999). The continuing importance of bile acids in liver and intestinal disease. *Archives of Internal Medicine*, *159*(22), 2647-2658.

Hughes, M.P. (2016). Fifty years of dielectrophoretic cell separation technology. *Biomicrofluidics*, *10*(3). https://doi.org/10.1063/1.4954841

International Agency for Research on Cancer (2013, December). *Latest world cancer statistics, global cancer burden rises to 14.1 million new cases in 2012: marked increase in breast cancers must be addressed*. (Publication No. PR 223). Retrieved from http://www.iarc.fr/en/media-centre/pr/2013/pdfs/pr223_E.pdf

International Agency for Research on Cancer (2014). GLOBOCAN 2012: Estimated cancer incidence, mortality and prevalence worldwide in 2012. Retrieved from http://globocan.iarc.fr/Pages/fact_sheets_population.aspx#

Jiang, W.G., Sanders, A.J., Katoh, M., Ungefroren, H., Gieseler, F., Prince, M., …Santini, D. (2015). Tissue invasion and metastasis: molecular, biological and clinical perspectives. *Seminars in Cancer Biology*, *35*, 244-275.

John, A.S., & Price, C.P. (2013). Economic evidence and point-of-care testing. *The Clinical Biochemist Reviews*, *34*, 61-74.

Kardum, N., Petrovic-Oggiano, G., Takic, M., Glibetic, N., Zec, M., Debeljak-Martacic, J., & Konic-Ristic, A. (2014). Effects of glucomannan-enriched, Aronia juice-based supplement on cellular antioxidant enzymes and membrane lipid status in subjects with abdominal obesity. *The Scientific World Journal*. http://dx.doi.org/10.1155/2014/869250

Katsuraya, K., Okuyama, K., Hatanaka, K., Oshima, R., Sato, T., & Matsuzaki, K. (2003). Constitution of konjac glucomannan: chemical analysis and $^{13}C$ NMR spec-troscopy. *Carbohydrate Polymers*, *53*(2), 183-189.

Keithley, J.K., Swanson, B., Mikolaitis, S.L., DeMeo, M., Zeller, J.M., Fogg, L., & Adamji, J. (2013). Safety and efficacy of glucomannan for weight loss in overweight and moderately obese adults. *Journal of Obesity*. http://dx.doi.org/10.1155/2013/610908

Klinder, A., Forster, A., Caderni, G., Femia, A.P., & Pool-Zobel, B.L. (2004). Fecal water genotoxicity is predictive of tumour-preventive activities by inulin-like oligofructoses, probiotics (*Lactobacillus rhamnosus* and *Bifidobacterium lactis*), and their symbiotic combination. *Nutrition and Cancer*, *49*(2), 144-155.

Kohno, T., & Yokota, J. (1999). How many tumour suppressor genes are involved in human lung carcinogenesis? *Carcinogenesis*, *20*(8), 1403-1410.

Kritchevsky, D. (1987). Dietary fibre and lipid metabolism. *International Journal of Obesity*, *11*(1), 33-43.

Kudo, M. (2015). Surveillance, diagnosis, treatment and outcome of liver cancer in Japan. *Liver Cancer*, *4*, 39-50.

Kumar, S., Kamboj, J., & Suman, S. (2011). Overview for various aspects of the health benefits of Piper longum linn. fruit. *Journal of Acupuncture and Meridian Studies*, *4*(2), 134-140.

Lattimer, J.M., & Haub, M.D. (2010). Effects of dietary fibre and its components on metabolic health. *Nutrients*, *2*. 1266-1289.

Lee, J.K., Kim, J.H., & Shin, H.K. (2011). Therapeutic effects of the oriental herbal medicine Sho-saiko-to on liver cirrhosis and carcinoma. *Hepatology Research*, *41*(9), 825-837.

Li, J., & Cheng, J.X. (2014). Direct visualisation of *de novo* lipogenesis in single living cells. *Scientific Reports*, *4*. Retrieved from http://www.nature.com/articles/srep06807

Llovet, J.M., Fuster, J., & Bruix, J. (2004). The Barcelona approach: diagnosis, staging, and treatment of hepatocellular carcinoma. *Liver Transplantation*, *10*(2), 115-120.

Magnatong, L., Ko, P.J., & Dixon, S.J. (2016). Emerging roles for lipids in non-apoptotic cell death. *Cell Death & Differentiation*, *23*, 1099-1109.

Maor, Y., & Malnick, S. (2013). Liver injury induced by anticancer chemotherapy and radiation therapy. *International Journal of Hepatology*. http://dx.doi.org/10.1155/2013/815105

Marur, S., & Forastiere, A.A. (2010). Challenges of integrating chemotherapy and targeted therapy with radiation in locally advanced head and neck squamous cell cancer. *Current Opinion in Oncology*, *22*(3), 206-211.

Masuda, S., Washizu, M., & Nanba, T. (1989). Novel method of cell fusion in field constriction area in fluid integration circuit. *IEEE Transactions on Industry Applications*, *25*(4): 732-737.

Merriam, S., & Muhamad, M. (2013). Roles traditional healers play in cancer treatment in Malaysia: implications for health promotion and education. *Asian Pacific Journal of Cancer Prevention*, *14*(6), 3593-3601.

Mersch-Sundermann, V., Knasmuller, S., Wu, X.J., Darroudi, F., & Kassie, F. (2004). Use of a human-derived liver cell line for the detection of cytoprotective, antigenotoxic and cogenotoxic agents. *Toxicology*, *198*(1-3), 329-340.

Mulhall, H.J., Labeed, F.H., Kazmi, B., Costea, D.E., Hughes, M.P., & Lewis, M.P. (2011). Cancer, pre-cancer and normal oral cells distinguished by dielectrophoresis. *Analytical and Bioanalytical Chemistry, 401*(8), 2455–2463.

Multani, A.S., & Chang, S. (2007). WRN at telomeres: implications for aging and cancer. *Journal of Cell Science*, *120*, 713-721.

Nam, D., Barrack, R.L., & Potter, H.G. (2014). What are the advantages and disadvantages of imaging modalities to diagnose wear-related corrosion problems? *Clinical Orthopaedics and Related Research, 472*, 3665-3673.

Naseri, M.H., Mahdavi, M., Davoodi, J., Tackallou, S.H., Goudarzvand, M., & Neishabouri, S.H. (2015). Up regulation of Bax and down regulation of Bcl 2 during 3-NC mediated apoptosis in human cancer cells. *Cancer Cell International, 15*(55). https://doi.org/10.1186/s12935-015-0204-2

Nastruzzi, C., Tosi, A., Borgatti, M., & Guerrieri, R. (2007). CMOS Biotechnology. In D. Ham & R.M. Westervelt (Eds). *Applications of dielectrophoresis-based lab-on-a-chip devices in pharmaceutical sciences and biomedicine* (pp. 145-178). Retrieved from http://www.springerlink.com/index/l31km2ljrk2gh688.pdf

Nolan, T., Hands, R.E., & Bustin, S.A. (2006). Quantification of mRNA using real-time RT-PCR. *Nature Protocols*, *1*, 1559-1582.

Norsa'adah, B., & Zayani, C.G.N. (2013). Epidemiology and survival of hepatocellular carcinoma in north-east Peninsular Malaysia. *Asian Pacific Journal of Cancer Prevention, 14*(11), 6955-6959.

Ozkan, M., Pisanic, T., Scheel, J., Barlow, C., Esener, S., & Bhatia, S.N. (2003). Electro-optical platform for manipulation of live cells. *Langmuir, 19*(5), 1532-1538.

Pethig, R., & Kell, D.B. (1987). The passive electrical properties of biological systems: their significance in physiology, biophysics and biotechnology. *Physics in Medicine and Biology, 32*(8), 933-970.

Pohl, H.A. (1951). The motion and precipitation of suspensoids in divergent electric fields. *Journal of Applied Physics*, *22*(7), 869-871.

Pohl, H.A., & Hawk, I. (1966). Separation of living and dead cells by dielectrophoresis. *Science*, *152*(3722), 647-649.

Prakash, O., Kumar, A., Kumar, P., & Ajeet (2013). Anticancer potential of plants and natural products: a review. *American Journal of Pharmacological Sciences*, *1*(6), 104-115.

Raza, A., & Soob, G.K. (2014). Hepatocellular carcinoma review: current treatment, and evidence-based medicine. *World Journal of Gastroenterology*, *20*(15), 4115-4127.

Roberti, A., La Sala, D., & Cinti, C. (2006). Multiple genetic and epigenetic interacting mechanisms contribute to clonally selection of drug-resistant tumours: current views and new therapeutic prospective. *Journal of Cellular Physiology*, *207*(3), 571-81.

Romagosa, C., Simonetti, S., Lopez-Vincente, L., Mazo, A., Lleonart, M.E., Castellvi, J., & Cajal, S.R. (2011). $p16^{Ink4a}$ overexpression in cancer: A tumour suppressor gene associated with senescence and high-grade tumours. *Oncogene*, *30*, 2087-2097.

Saar, B., & Kellner-Weldon, F. (2008). Radiological diagnosis of hepatocellular carcinoma. *Liver International*, *28*(2), 189-199.

Safa, A.R. (2016). Resistance to cell death and its modulation in cancer stem cells. *Critical Reviews in Oncogenesis*, *21*(3-4), 203-219.

Sampathkumar, S.G., Jones, M.B., Meledeo, M.A., Campbell, C.T., Choi, S.S., Hida, K., …Yarema, K.J. (2006). Targeting glycosylation pathways and the cell cycle: sugar-dependent activity of butyrate-carbohydrate cancer prodrugs. *Chemistry & Biology*, *13*(12), 1265-1275.

Sebti, S.M., & Hamilton, A.D. (2000). Design of growth factor antagonists with antiangiogenic and antitumour properties. *Oncogene*, *19*(56), 6566-6573.

Shah, B.R., Li, B., Wang, L., Liu, S., Li, Y., Wei, X., …Li, Z. (2015). Health benefits of konjac glucomannan with special focus on diabetes. *Bioactive Carbohydrates and Dietary Fibre*, *5*(2), 179-187.

Shahbuddin, M., Shahbuddin, D., Bullock, A.J., Ibrahim, H., Rimmer, S., & MacNeil, S. (2013). High molecular weight plant heteropolysaccharides stimulate fibroblasts but inhibit keratinocytes. *Carbohydrate Research*, *375*, 90-99.

Shaikh, S.R., & Edidin, M. (2008). Polyunsaturated fatty acids and membrane organisation: the balance between immunotherapy and susceptibility to infection. *Chemistry and Physics of Lipids*, *153*(1), 24-33.

Shay, J.W., & Wright, W.E. (2002). Telomerase: a target for cancer therapeutics. *Cancer Cell*, *2*(4), 257-265.

Signorelli, P., Croce, P., & Dede, A. (1996). A clinical study of the use of a combination of glucomannan with lactulose in the constipation of pregnancy. *Minerva Ginecologica*, *48*(12), 577-582.

Silva, I.D.S. (1999). *Cancer epidemiology: principles and methods* [International Agency for Research on Cancer]. Retrieved from https://books.google.com.my

Srikaeo, K., & Singchai, J. (2016). Effects of konjac glucomannan and resistant starch on in vitro lipid digestion of non-dairy creamers. *International Food Research Journal*, *23*(4), 1403-1408.

St Croix, B., Sheehan, C., Rak, J.W., Florenes, V.A., Slingerland, J.M., & Kerbel, R.S. (1998). E-cadherin-dependent growth suppression is mediated by the cyclin-dependent kinase inhibitor p27(KIP1). *The Journal of Cell Biology*, *142*(2), 557-571.

Stein-Gerlach, M., Wallasch, C., & Ultrich, A. (1998). SHP-2, SH2-containing protein tyrosine phosphatase-2. *The International Journal of Biochemistry & Cell Biology*, *30*(5), 559-566.

Story, J.A., Furumoto, E.J., & Buhman, K.K. (1997). Dietary fibre and bile acid metabolism - an update. *Advances in Experimental Medicine and Biology*, *427*, 259-266.

Stowell, S.R., Ju, T., & Cummings, R.D. (2015). Protein glycosylation in cancer. *Annual Review of Pathology*, *10*, 473-510.

Takashima, T., Matsui, O., Suzuki, M., & Ida, M. (1982). Diagnosis and screening of small hepatocellular carcinomas. Comparison of radionuclide imaging, ultrasound, computed tomography, hepatic angiography, and α1-fetoprotein assay. *Radiology*, *145*, 635-638.

Van Meerloo, J., Kaspers, G.J.L., & Cloos, J. (2011). *Cancer Cell Culture Methods and Protocols*. New York, NY: Humana Press.

Wang, X.Q., Ongkeko, W.M., Chen, L., Yang, Z.F., Lu, P., Chen, K.K., …Fan, S.T. (2010). Octamer 4 (Oct4) mediates chemotherapeutic drug resistance in liver cancer cells through a potential Oct4-AKT-ATP-binding cassette G2 pathway. *Hepatology*, *52*(2), 528-539.

Weng, P.Y., Chen, I.A., Yeh, C.K., Chen, P.Y., & Juang, J.Y. (2016). Size-dependent dielectrophoretic crossover frequency of spherical particles. *Biomicrofluidics*, *10*(1). https://doi.org/10.1063/1.4941853

Widjanarko, S.B., Wijayanti, N., & Sutrisno, A. (2013). Laxative potential of the konjac flour (*Amorphophallus muelleri* Blume) in treatment of loperamide induced constipation on Sprague Dawley rats. *International Journal of Medical and Health Sciences*, *7*(11), 729-733.

Wong, R.J., Cheung, R., & Ahmed, A. (2014). Nonalcoholic steatohepatitis is the most rapidly growing indication for liver transplantation in patients with hepatocellular carcinoma in the U.S. *Hepatology*, *59*(6), 2188-2195.

Wu, W.T., & Chen, H.L. (2011). Konjac glucomannan and inulin systematically modulate antioxidant defence in rats fed a high-fat fibre-free diet. *Journal of Agricultural and Food Chemistry*, *59*(17), 9194-9200.

Wu, W.T., Cheng, H.C., Chen, H.L. (2011). Ameliorative effects of konjac glucomannan on human faecal β-glucuronidase activity, secondary bile acid levels and faecal water toxicity Caco-2 cells. *British Journal of Nutrition*, *105*(4), 593-600.

Wu, Z., Lu, Y., Wang, B., Liu, C., & Wang, Z.R. (2003). Effects of bile acids on proliferation and ultrastructural alteration of pancreatic cancer cell lines. *World Journal of Gastroenterology*, *9*(12), 2759-2763.

Xin, C., Chen, J., Liang, H., Wan, J., Li, J., & Li, B. (2017). Confirmation and measurement of hydrophobic interaction in sol-gel system of konjac glucomannan with different degree of deacetylation. *Carbohydrate Polymers*, *174*, 337-342.

Yafouz, B., Kadri, N.A., & Ibrahim, F. (2012). The design and simulation of a planar microarray dot electrode for a dielectrophoretic lab-on-chip device. *International Journal of Electrochemical Science*, *7*, 12054-12063.

Yafouz, B., Kadri, N.A., & Ibrahim, F. (2013). Microarray dot electrodes utilizing dielectrophoresis for cell characterization. *Sensors*, *13*(7), 9029-9046.

Yafouz, B., Kadri, N.A., & Ibrahim, F. (2014). Dielectrophoretic manipulation and separation of microparticles using microarray dot electrodes. *Sensors*, *14*(4), 6356-6369.

Yafouz, B., Kadri, N.A., Rothan, H.A., Yusof, R., & Ibrahim, F. (2016). Discriminating dengue-infected hepatic cells (WRL-68) using dielectrophoresis. *Electrophoresis*, *37*(3), 511-518.

Yaswen, P., MacKenzie, K.L., Keith, W.N., Hentosh, P., Rodier, F., Zhu, J., …Yang, X. (2015). Therapeutic targeting of replicative immortality. *Seminars in Cancer Biology*, *35*, 104-128.

Yin, Y., & Shen, W.H. (2008). PTEN: a new guardian of the genome. *Oncogene*, *27*, 5443-5453.

Yuen, M.F., Cheng, C.C., Lauder, I.J., Lam, S.H., Ooi, C.G.C., & Lai, C.L. (2000). Early detection of hepatocellular carcinoma increases the chance of treatment: Hong Kong experience. *Hepatology*, *31*(2), 330-335.

Zhao, L., Guo, X., Wang, O., Zhang, H., Wang, Y., Zhou, F., …Ji, B. (2016). Fructose and glucose combined with free fatty acids induce metabolic disorders in HepG2 cell: a new model to study the impacts of high-fructose/sucrose and high-fat diets *in vitro*. *Molecular Nutrition & Food Research*, *60*(4), 909-921.

Zhao, Y.J., Ju, Q., & Li, G.C. (2013). Tumour markers for hepatocellular carcinoma (review). *Molecular and Clinical Oncology*, *1*, 593-598.

Zhu, H.H., Luo, X., Zhang, K., Cui, J., Zhao, H., Ji, Z., …Feng, G.S. (2015). Shp2 and Pten have antagonistic roles in myeloproliferation but cooperate to promote erythropoiesis in mammals. *Proceedings of the National Academy of Sciences of the United States of America*, *112*(43), 13342-13347.

Ziyad, S., & Iruela-Arispe, M.L. (2011). Molecular mechanisms of tumour angiogenesis. *Genes Cancer*, *2*(12), 1085-1096.

## SUPPLEMENTARY

### List of publications and paper presented

1. Sawai, S., Mohktar, M.S., Wan Safwani, W.K.Z., & Ramasamy, T.S. (2018). Suppression of the viability and proliferation of HepG2 hepatocellular carcinoma cell line by konjac glucomannan. *Anti-cancer Agents in Medicinal Chemistry*, *18*(9), 1258-1266. (Published article) (Appendix A)
2. Sawai, S., Mohktar, M.S., Wan Safwani, W.K.Z., & Ramasamy, T.S. (2016). *Cytotoxic effect of konjac glucomannan on HepG2 and WRL68 cell lines*. *Proceedings Book of 6th Malaysian Tissue Engineering and Regenerative Medicine Scientific Meeting (MTERMS) and 2nd Malaysian Stem Cell Meeting held on November 17-18, 2016 at The Light Hotel, Penang, Malaysia* (pp. 19). (Published conference abstract) (Appendix B)